nature portfolio

Peer Review File

Pro-efferocytic nanotherapies reduce vascular inflammation without inducing anemia in a large animal...

REVIEWER COMMENTS

Reviewer #1 (Remarks to the Author):

In the manuscript entitled "Pro-efferocytic nanotherapies reduce vascular inflammation without inducing anemia in a large animal model of atherosclerosis" by Bamezai el al., the authors describe the use of a macrophage-specific nanotherapy to deliver a chemical inhibitor of an effector molecule downstream of CD47 to treat atherosclerosis in a porcine model of atherosclerosis. This pro-effercytotic nanotherapy was found to reduce apoptosis and stimulate anti-inflammatory changes in atherosclerotic plaques without inducing anemia, which is associated with CD47 blockade. While the use of both a large animal model and an emerging therapeutic modality greatly increases the clinical relevance of this treatment and the studies presented in this manuscript are thought-provoking, there are a number of scientific and conceptual concerns that reduce enthusiasm for this submission. Despite these concerns, the results do support the conclusions and the study represents an important step in producing a novel approach to treat a medical condition that despite being the focus of intense research resources effort, have not produced many new treatment options.

Major concerns:

1. The LDLR1 null porcine model utilizes young animals that are fed a "Western diet" for 12 weeks, which represents an early time in the progression of atherosclerosis and development, which would not closely comport with the most common situation in humans where diagnosis of plaque burden would be made at a more advanced state of disease and at in older people. While the findings are promising and the expense of these experiment is understandably high, the findings presented here would be far more impressive if the authors used a more advanced disease stage and in older animals; some of which were converted to a "Normal diet" at the onset of treatment.

2. Does the synthesis of single-walled carbon nanotubes follow current good manufacturing practices for therapeutic agents? Obviously, implementation of these quality assurance practices would be required prior to the initiation of human trials. Despite this reservation, the authors did show SWNTs were nearly exclusively taken up by inflammatory monocytes and macrophages.

3. The integration of bulk RNA sequencing results from the current pig study with single cell RNA sequencing results from a

previously published mouse intervention study seems unusual as the progression of atherosclerosis in these models would likely be significantly different.

4. While the authors show that pro-efferocytic, macrophage-selective nanoparticles can be generated at scale to reduce vascular inflammation in a large animal model of atherosclerosis initiation, the translation of this technology may be impeded by the anticipated expense.

Minor concerns:

1. The image quality of some of the figures is sub-standard and should be improved.

2. While 18F-FDG is commonly used to indicate increased cellular activity that can result from infection or inflammation, the uptake of glucose can occur for a variety of other reasons, which should be clarified in the text.

Reviewer #2 (Remarks to the Author):

In this work, the authors achieved scale-up production of nanoparticles based on previously developed macrophage-specific nanotherapeutics and validated the therapeutic potential of nanoparticles for early atherosclerosis in pigs. This is a promising treatment for atherosclerosis and can be expanded to other inflammatory diseases. It is recommended for publication in Nature Communication with the following modifications.

1. Why does an acidic environment accelerate the release of SHP1. Please explain the mechanism further.

2. The UV-visible absorption spectrum in Fig. 1b is not consistent with previously reported small-scale products (Nature Nanotechnology, 15, 154–161 (2020)), and no significant absorption peaks for Cy 5.5 are seen in the figure. The authors are advised to explain this concern.

3. Although SWNT-SHP1i also has good atherosclerotic therapeutic effects in pigs, there is no evidence in this study to directly confirm that SWNT-SHP1i achieves effective enrichment at atherosclerotic plaque sites. This is a hindrance to exploring the therapeutic mechanism of SWNT-SHP1i.

4. Multiple flow results showed that SWNT-SHP1i was preferentially taken up by inflammatory monocytes and macrophages, either in the circulation or within plaques. What factors mediate the occurrence of this specific endocytosis?

5. The paper only shows blood safety during long-term treatment with different materials, but there are no blood samples from the diseased and healthy groups to serve as controls. Long-term drug treatment inevitably triggers chronic damage to the organism, and I believe it is necessary to observe various blood indices in healthy pigs to further ensure the long-term biosafety of SWNT-SHP1i.

6. Does the loading rate of SHP1i change in mass-produced SWNT-SHP1i?

Reviewer #3 (Remarks to the Author):

Major Comments

The authors have previously reported that reactivating efferocytosis, the process by which macrophages phagocytose inflamed cells, holds promise for translational research in atherosclerotic cardiovascular disease. They have shown that blocking CD47 can reduce plaque burden by enhancing the clearance of apoptotic vascular tissue. However, it's important to note that systemic CD47 blocking can lead to anemia, necessitating clinical attention.

In this study, the authors introduce the concept of a "Trojan horse" macrophage-specific nanotherapy and test it in an LDLR-/- porcine model of atherosclerosis. Their aim is to determine whether this approach justifies further investigation in human clinical trials. Notably, their research extends their previous work conducted in a murine model of atherosclerosis, demonstrating the scalability and translational potential of their findings. In the early stages of the disease, their pro-efferocytic nanotherapy effectively reduces the accumulation of apoptotic cells and induces anti-inflammatory changes within the plaque.

1. The FACS analysis results to support that SWNTs are preferentially taken up by monocytes in the circulation lack rigor. It's important to include an overall percentage of all immune cells detected, along with the frequency of SWNT+ and SWNT- cells in each population. Additionally, the spectral unmixing model should be validated with compensation controls, and spectral fluorescence signature data of stained and unstained samples should be provided.

2. In Figure 2, there are concerns about legibility and clarity:

- The axis labels need adjustment for improved readability.

- The directionality of the populations of interest, including the singlets suggesting the CD21+ and CD3-CD21- populations (NK population), should be clarified for better understanding.

- It would be beneficial to include data on the overall percentage of major immune cell types in the model, especially the monocyte percentage and T cell percentages before and after SWNT uptake.

- Given that flow cytometry was performed with whole blood samples, the percentage of neutrophils and their potential role in nanoparticle uptake should be discussed.

3. CBC should include the leukocyte count results, which are part of the standard test.

4. The authors should provide clearer information about which animals were used for each experiment.

5. In Figure 3:

- The gating strategy, particularly the shape of the gating shown in the representative figure, is not clear. An unstained control should be included to justify the gating.

- Figure 3d: It should be clarified whether the ORO histology was performed in mice or pigs. Additionally, the scale bar is not visible.

- The scale bar is missing in most representative figures.

6. In Figure 3c, bar plots should include dots. It is concerning that only two pigs per group were analyzed, raising statistical concerns.

7. Figure 4's RNA seq analysis lacks attention to detail. The integration methods for RNA seq are not described, and the volcano plot does not allow proper visualization of genes. The Venn diagram mentions that >40 genes overlap between species, but only 10 are listed.

8. In Figure 4, the GO enrichment and pathway analysis should include pathways related to efferocytosis. The GO terms for heme metabolism and alterations in neutrophil activation should be addressed. The presence of several genes related to scavenger receptors, solute carrier transporters, and immune cell activation should also be discussed.

Minor Comments

1. In Figure 1, the legend should explain the meaning of T% (Fig. 1c).

Reviewer #4 (Remarks to the Author):

In the submitted manuscript, Bamezai et al. upscale and test a nanoparticle-based experimental therapy to block CD47-induced signaling in macrophages in LDL receptor knockout minipigs. In a previous elegant study in mice, the group showed that these nanoparticles could reduce atherosclerosis, stimulate phagocytosis of apoptotic remnants, and reduce necrotic core size. The effort to translate this promising approach toward clinical studies by testing it in a large animal model is laudable. Unfortunately, however, the authors do not obtain clear positive results with respect to the efficient loading of monocytes in blood or its effects on atherosclerosis, which is only studied at a very early stage. Furthermore, 3 out of 14 pigs died of which 2 may have been nanoparticle-related deaths.

Major issues

1. Figure 1. It is concluded in the text that 78%/42% CD163+CD14- are positive for the nanoparticles, but these are fractions of rare cell populations. For the much more abundant CD14+ CD163- population, the fraction is only a few percent, raising questions about whether this is enough to have any impact. The fraction is much less than in the authors' previous paper in mice (ref 11). If the reason is a problem in detection, there may be no way around doing at least some fluorophore-coupled studies. It would also be helpful to discuss how these monocyte subgroups compare to those of the mouse studies.

2. Figure 2. If pieces of straight segments of the carotid artery are used, they are not likely to contain any atherosclerosis at this early stage of plaque development, because the straight segments of common carotid arteries are not atherosclerosis-prone regions. In that case, the cells should not be referred to as intraplaque cells.

3. Figure 3. There are only very early changes in the intima and the authors should avoid calling this atherosclerotic plaque. However, it would be highly interesting to test this therapy in animals with proper atherosclerotic plaques, and this should be possible as an intervention trial after plaques are induced by long-term high-fat diet feeding.

4. Figure 3e. A critical requirement for the t-test is that observations are independent, but they are not in this case, where each animal contributes two data points. This inflates the type 1 error. Instead, the average should be used which would mean n=5 in each group, and therefore likely no statistical difference. Please also report signal intensities from a neighboring vein or the heart ventricles to demonstrate that carotid SUV differences are not coming from background differences.

5. Figure 3f. There is no significant change in intimal macrophages. Concluding that there is a trend at p=0.46 seems unjustified.

5. Figure 3g. It is surprising that the small dots can amount to 3 percent of the lesion area, and it would in any case be a better measure to count Tunel/Dapi+ signal and provide the ratio against total Dapi+ cells. Also, please note that for the statistical test used, the assumption of equal variance in the t-test is not fulfilled.

6. If slower infusion of the therapy has been part of the solution for avoiding the pigs dying on the operating table, the authors should consider whether they are caused by the CARPA reaction, which is often observed in pigs after the infusion of nanoparticles.

Minor issues

1. Figure 1. The small graphs at the top showing which subpopulation is being examined appear to be switched in some cases. Furthermore, it would be helpful with some kind of explanation of how the SWNT gate is set and why it looks different in the different analyses.

2. Figure 2. Please explain how the gate for SWNT+ cells was set.

3. In the methods description for the pigs, it is written as if the gene modification was created anew in this batch of pigs, but they were probably bred from gene-modified founders. Please clarify.

4. Figure 3d. Mice are mentioned.

Reviewer #1 (Remarks to the Author):
In the manuscript entitled "Pro-efferocytic nanotherapies reduce vascular inflammation without inducing anemia in a large animal model of atherosclerosis" by Bamezai el al., the authors describe the use of a macrophage-specific nanotherapy to deliver a chemical inhibitor of an effector molecule downstream of CD47 to treat atherosclerosis in a porcine model of atherosclerosis. This pro-effercytotic nanotherapy was found to reduce apoptosis and stimulate anti-inflammatory changes in atherosclerotic plaques without inducing anemia, which is associated with CD47 blockade. While the use of both a large animal model and an emerging therapeutic modality greatly increases the clinical relevance of this treatment and the studies presented in this manuscript are thought-provoking, there are a number of scientific and conceptual concerns that reduce enthusiasm for this submission. Despite these concerns, the results do support the conclusions and the study represents an important step in producing a novel approach to treat a medical condition that despite being the focus of intense research resources effort, have not produced many new treatment options.

Major concerns:
1. The LDLR1 null porcine model utilizes young animals that are fed a "Western diet" for 12 weeks, which represents an early time in the progression of atherosclerosis and development, which would not closely comport with the most common situation in humans where diagnosis of plaque burden would be made at a more advanced state of disease and at in older people. While the findings are promising and the expense of these experiment is understandably high, the findings presented here would be far more impressive if the authors used a more advanced disease stage and in older animals; some of which were converted to a "Normal diet" at the onset of treatment.

Response: *We thank the Reviewer for making these suggestions and agree that repeating our study in a more advanced disease model would support and strengthen our current findings. However, the cost of this work would be prohibitive for an academic group like ours, without support beyond that which is available from traditional funding sources like the NIH.*

For example, simply extending our study from 3 months to 6 months (even with a modest sample size of n=8/condition) would cost an additional: $211,866 in pig procurement/housing/Western diet fees, $262,669 in unlabeled SWNT manufacturing costs, ~$45,000 in transportation and PET/CT imaging fees, and ~$72,000 in veterinary service, anesthesia, phlebotomy and laboratory fees, for a grand total of ~$591,535 (exclusive of salary support for our post-doc team). If we wished to add a Cy5.5 molecular imaging probe (which costs an additional $9,520/dose/pig), the total cost of the experiment would rapidly exceed $1M. The remarkable cost associated with this work is driven by the rapid weight gain experienced by these animals as they age, and scaling of the therapeutic reagents (which are dosed per kg). So, while we very much hope to be able to conduct such a study in the future, we believe this will only be possible once our initial findings are disseminated and we can attract the support of an industry partner able to advance our work into a large animal model at a later stage of disease, and then into human trials.

2. Does the synthesis of single-walled carbon nanotubes follow current good manufacturing practices for therapeutic agents? Obviously, implementation of these quality assurance practices would be required prior to the initiation of human trials. Despite this reservation, the authors did show SWNTs were nearly exclusively taken up by inflammatory monocytes and macrophages.

Response*: We appreciate Reviewer #1's question as it highlights an important criterion necessary for translation into human clinical trials. We agree that implementation of GMP quality assurance practices will be critical for this next step. Because our university, like many other academic centers, is not equipped with GMP-certified nanoparticle manufacturing facilities, we attempted to approximate such manufacturing practices wherever possible. For example, all SWNTs were generated using sterile*

techniques with testing for contamination. Other quality control measures such as screening for the presence of endotoxin were also conducted. Physiochemical characterization was performed with each synthesized batch using dynamic light scattering, UV-Vis spectroscopy, and often FT-IR spectroscopy to validate nanoparticle size, zeta potential, chemical properties, and consistency over the course of the experiment (Figure 1). We are currently communicating with a private biotechnology company interested in advancing this work into the clinic and are discussing how to generate clinical-grade material with them in a GMP-compliant fashion.

3. The integration of bulk RNA sequencing results from the current pig study with single cell RNA sequencing results from a previously published mouse intervention study seems unusual as the progression of atherosclerosis in these models would likely be significantly different.

Response: *We appreciate the Reviewer's comment about the integrated RNA sequencing data, and the opportunity to explain our rationale for doing so. We agree that the models do not perfectly overlap, and may potentially reflect different stages of atherogenesis, in addition to differences across species. However, we felt that searching for genes and pathways that are consistently modulated between experiments could be a useful way to build confidence in our results. Accordingly, we originally presented those DEGs and GO pathways which were commonly up- and down-regulated in each species, which we viewed as high-confidence findings that might persist in humans, should our work be translated into the clinic.*

*However, we agree with the Reviewer that it may not be entirely appropriate to integrate RNAseq findings from different species, and we now present the pig data both separately and in combination with our murine findings. Differentially expressed genes from the pig bulk RNA sequencing data set are now provided in Supplemental Table 1, which demonstrates upregulation of genes implicated in both atherosclerosis and inflammatory pathways. For reference, the top 20 labeled DEGs are included below (**Revision Table A**). Similarly, the GO pathway analysis of the pig bulk RNA-sequencing was rerun using the newly released PANTHER Overrepresentation Test (Released 02/26/2024), which implicated pathways involved in the immune system and defense response, response to external stimuli, endocytosis, phagocytosis, and cytokine production (please see **Manuscript Supplemental Figure 5** below). Integrating this dataset with the mouse scRNA-seq data (cluster 1 - monocyte and cluster 4 - macrophage subpopulations) narrowed these lists and provided insight into 35 shared DEGs that further highlight the role of SWNT-SHP1i nanotherapy in the immune system response, response to an external biotic stimulus, endocytosis, and phagocytosis (please see below **Supplemental Figure A**). We believe that presenting both analyses (pig-only and integrated) has strengthened the revised manuscript, but we are happy to remove the cross-species results if the Reviewer believes that would be more appropriate.*

Gene ID	log2FoldChange	p. adj	Gene Name
ENSSSCG00000002782	5.63	0.01	PLEKHG4
ENSSSCG00000039745	4.98	2.09E-03	HMOX1
ENSSSCG00000039798	4.49	3.70E-03	SLC11A1
ENSSSCG00000056276	4.28	0.04	SLAMF9
ENSSSCG00000038688	3.90	4.54E-04	PGLYRP1
ENSSSCG00000028331	3.90	0.04	IL1R2
ENSSSCG00000025993	3.62	0.04	SGPP2
ENSSSCG00000002032	3.50	9.69E-04	SLC7A8
ENSSSCG00000032438	3.35	8.66E-05	FFAR2
ENSSSCG00000006588	3.34	0.04	S100A9
ENSSSCG00000029960	3.28	0.05	LRRC4B
ENSSSCG00000029414	3.21	0.01	FCN1
ENSSSCG00000038351	2.99	0.04	TNFRSF18
ENSSSCG00000062991	2.98	0.02	KCNK12
ENSSSCG00000036132	2.93	8.66E-05	CKM
ENSSSCG00000014259	2.87	0.01	ADAMTS19
ENSSSCG00000003846	2.81	0.04	GLIS1
ENSSSCG00000015246	2.81	0.01	ST14
ENSSSCG00000009929	2.78	2.15E-03	TRPV4
ENSSSCG00000021569	2.77	0.02	MMP25

Revision Table A. Pig bulk RNA-Sequencing top 20 DEGs sorted by descending fold change.

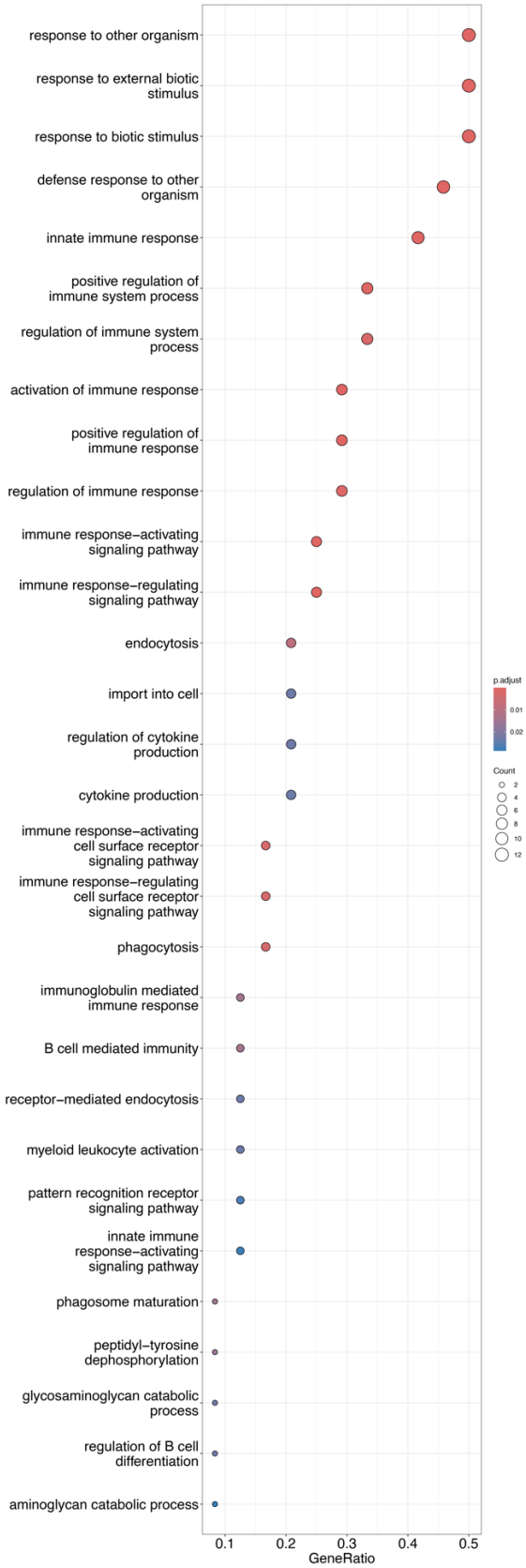

Revision Supplemental Figure 5. GO pathway analysis of Pig Bulk RNA-Sequencing

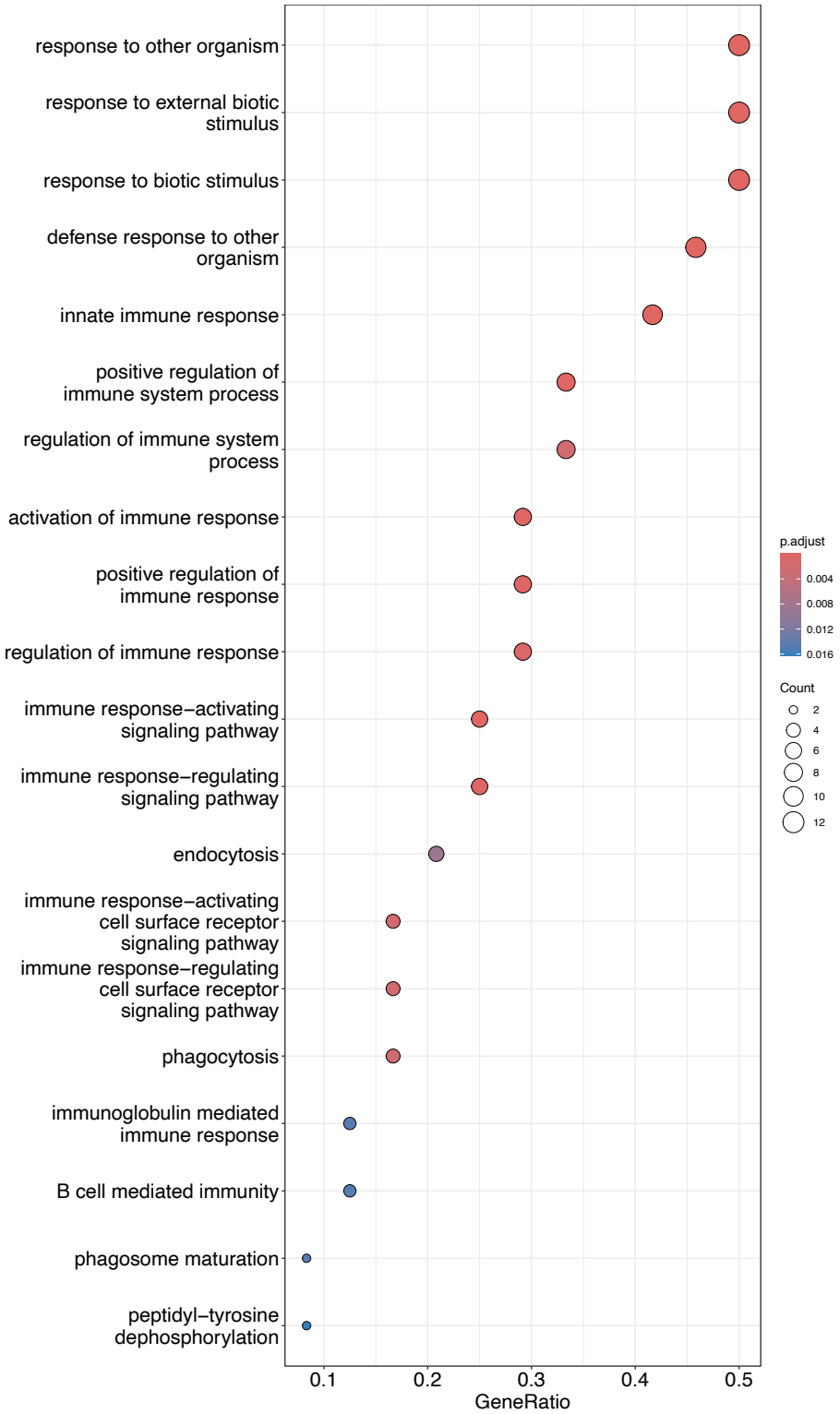

Figure A. Integrated Pig bulk RNA-Sequencing and Mouse scRNA-Sequencing GO Pathway Analysis of 35 shared DEGs (Top 20 GO pathways- Biological Process)

4. While the authors show that pro-efferocytic, macrophage-selective nanoparticles can be generated at scale to reduce vascular inflammation in a large animal model of atherosclerosis initiation, the translation of this technology may be impeded by the anticipated expense.

Response: *We completely agree with Reviewer #1's comment regarding the obstacle that price could represent as a barrier to translation of this therapeutic. Like any new technology, we hope that costs could fall as production is scaled up and manufacturing is performed by industrial chemists working outside of the academic setting. A key part of our scaling efforts to date has been to show that the nanoparticles continued to retain their uptake selectivity and pro-efferocytic efficacy after the costly molecular imaging probe Cy5.5 was removed. This simple change reduced our manufacturing costs by ~2/3 without apparent deleterious impact on the in vivo performance of the agent, representing an important translational advance. Given that most of the other ingredients of the nanoparticle are widely available from commercial vendors (e.g. raw carbon nanotubes and chemical SHP1 inhibitors), we anticipate that production costs will fall considerably once a commercial entity commits to building larger synthesis equipment (e.g. appropriate sonicators, etc.) compared to those available in our academic laboratories. Similar to price reductions seen with other recently introduced biologics such as PCSK9 inhibitors (which were initially listed for $14,000/year after their FDA approval in 2015, but were able to sustain a 60% price reduction by 2018)*[1,2]*, we are optimistic that our nanotherapy may become more affordable and accessible once professional manufacturing approaches replace those used by the authors in this preclinical study.*

Minor concerns:
1. The image quality of some of the figures is sub-standard and should be improved.

Response: *We agree with Reviewer #1's concern about the image quality, which we believe was, in part, a result of figure layout, image sizing, and font. We have modified the layout of Figure 3 by rearranging the subfigures, increasing the size of TUNEL and IBA1 histology images, increasing the font of the scale bar, and improving visualization of TUNEL*$^{+}$ *cells (see example in revised* ***Figure 3****). We have now updated the revised figure with magnified images of the TUNEL stain, as well. If additional changes are suggested, please do let us know.*

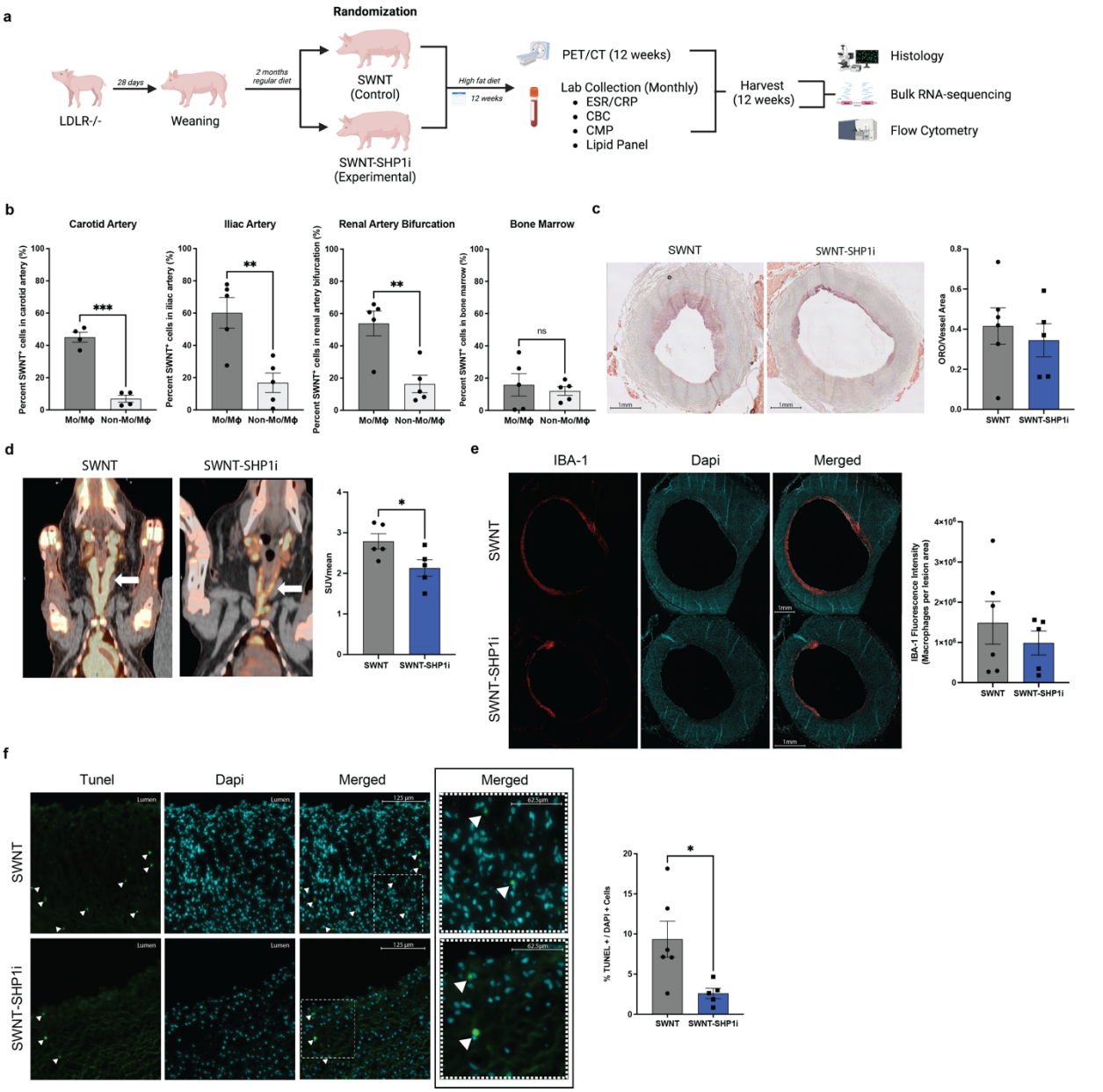

Revision Figure 3. SWNTs accumulate in atherosclerotic plaque and SHP1 inhibition reduces both vascular inflammation and apoptotic cell accumulation in transgenic atherosclerotic pigs, in vivo.

2. While 18F-FDG is commonly used to indicate increased cellular activity that can result from infection or inflammation, the uptake of glucose can occur for a variety of other reasons, which should be clarified in the text.

Response: *We appreciate and completely agree with Reviewer #1's comments. In our discussion of limitations within the revised manuscript, we now point out that ^{18}F-FDG can be impacted by a wide range of cellular processes in addition to vascular inflammation. In the discussion section, we now clarify: "FDG PET/CT plays a central role in the diagnosis of both oncologic and non-oncologic pathologies. While commonly associated with inflammation and infection, it is important to recognize that FDG PET signal is not specific for these phenomena and may be associated with unrelated triggers of glucose uptake within organs such as the brain, myocardium, and kidneys[3]."*

Reviewer #2 (Remarks to the Author):
In this work, the authors achieved scale-up production of nanoparticles based on previously developed macrophage-specific nanotherapeutics and validated the therapeutic potential of nanoparticles for early atherosclerosis in pigs. This is a promising treatment for atherosclerosis and can be expanded to other inflammatory diseases. It is recommended for publication in Nature Communication with the following modifications.

***Response**: We thank the Reviewer for these supportive comments and have attempted to address the residual concerns below.*

1. Why does an acidic environment accelerate the release of SHP1. Please explain the mechanism further.

***Response**: We thank the Reviewer for this question. At pH >7, SHP1i fairly stably interacts with the SWNTs via π-π electronic interactions. Under more acidic conditions (pH ~6.5 and 5.5), SHP1i release accelerates. This is because π-π stacking interactions are pH sensitive. Cyclohexadienedione on SHP1i may more likely protonate at acidic pH, which can increase aqueous solubility and interfere with π-π stacking interactions.*

2. The UV-visible absorption spectrum in Fig. 1b is not consistent with previously reported small-scale products (Nature Nanotechnology, 15, 154–161 (2020)), and no significant absorption peaks for Cy 5.5 are seen in the figure. The authors are advised to explain this concern.

***Response**: We appreciate the opportunity to explain this astute observation. The difference between the UV-Vis spectrum in this work and the published data in the 2020 Nature Nanotechnology paper is due to the scale of the optical density of the SWNT-SHP1i solution[4]. The solution OD tested in the present manuscript was 10-fold higher than that in the 2020 Nature Nanotechnology article, obscuring much of the peaks upon graph visualization. We have re-measured the UV-Vis curve of the SWNT-SHP1i reported herein using a similar OD to that used in our 2020 manuscript[4]. As shown below, the data display significant Cy5.5 and SHP1i peaks from the SWNT-SHP1i solution (**Figure B**). These new data are also provided in revised Figure 1b.*

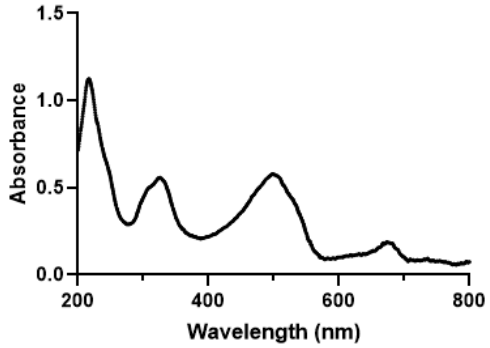

Figure B. UV-Vis of SWNT-SHP1i showing Cy5.5 peak at 674 nm and SHP1i peak at ~510 nm and 332 nm.

3. Although SWNT-SHP1i also has good atherosclerotic therapeutic effects in pigs, there is no evidence in this study to directly confirm that SWNT-SHP1i achieves effective enrichment at atherosclerotic plaque sites. This is a hindrance to exploring the therapeutic mechanism of SWNT-SHP1i.

***Response**: We thank the Reviewer for pointing out this limitation, and for the opportunity to address it experimentally. In the revised manuscript, we now provide flow cytometry data for the iliac artery, the renal artery bifurcation, and the bone marrow, in addition to that originally provided from the carotid artery (Figure 3b). This approach allows us to quantify differences in SWNT uptake between atherosclerotic vessels (e.g. the carotid artery, iliac artery, and renal artery bifurcation) and non-vascular tissue (e.g. the bone marrow). As shown below, we find limited SWNT-positivity in the non-monocyte/macrophage (MO/MΦ) populations in each of the three vascular tissue beds, consistent with prior findings indicating low uptake outside of these cell types. Similarly, we found very little SWNT uptake by MO/MΦ isolated from the bone marrow (~10%), consistent with the concept that our nanoparticle is not scavenged by mononuclear cells that are not inflamed. In contrast, we observed significant uptake in phagocytic cells isolated from the carotid arteries, iliac arteries, and the renal artery bifurcation (~4-5x more uptake than in MO/MΦ of the bone marrow), providing evidence for specific enrichment within the atherosclerotic plaque. These new data are now provided in the revised Manuscript Figure 3b and below in **Figure C**.*

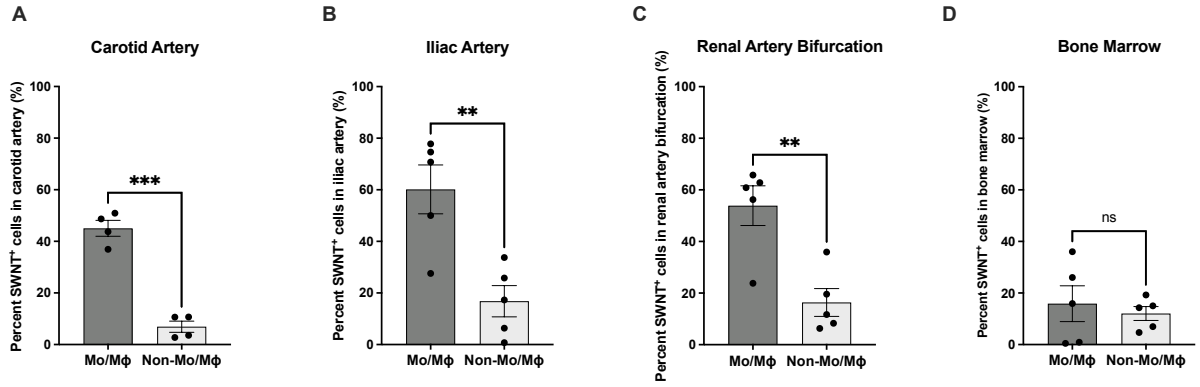

Figure C. SWNTs/SWNT-SHP1i were selectively taken up by the MO/MΦ population of vascular tissues containing atherosclerotic lesions as compared to similar populations from the bone marrow. A) SWNT$^+$ cells in the carotid artery (n=4, ***p=0.0001); B) SWNT$^+$ cells in the iliac artery (n=5, **p<0.01); C) SWNT$^+$ cells in the renal artery bifurcation (n=5, **p<0.01); D) SWNT$^+$ cells in the bone marrow (n=5, p=0.6314). Statistical analyses were performed using an unpaired T test with Welch's Correction.

*Because Reviewer 4 requested we include an experiment with a small cohort of animals treated with a short course (2 weeks) of fluorophore-labeled nanoparticles, we also took the opportunity to confirm the preceding flow cytometry results in this separate collection of animals. As shown below, specific enrichment in MO/MΦ from atherosclerotic vessels was again observed, further confirming our results highlighting concentration within the diseased blood vessel (**Figure D** shown as a Reviewer-only figure given the different timelines in each experiment).*

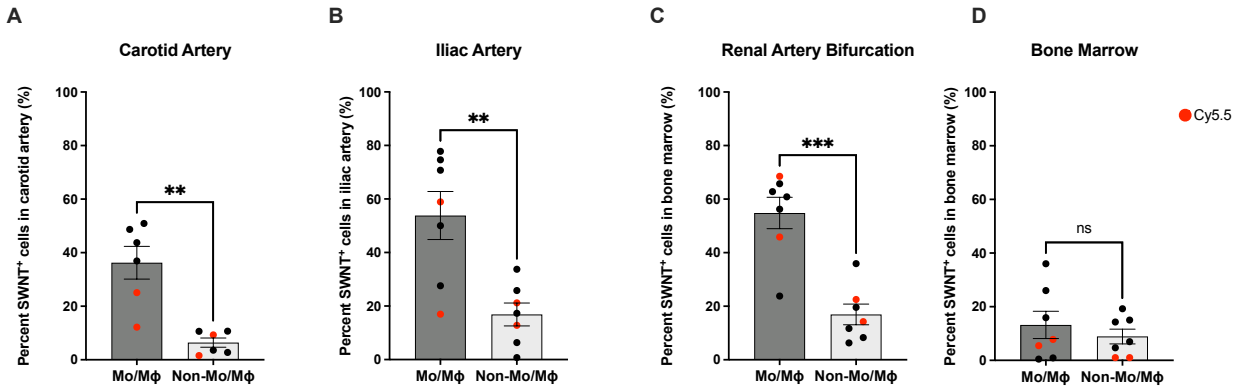

Figure D. SWNTs/SWNT-SHP1i were selectively taken up by the MO/MΦ population of vascular tissues containing atherosclerotic lesions as compared to a similar population of bone marrow cells. Cy5.5 tagged pigs treated with SWNT (n=1) or SWNT-SHP1i (n=1) for two weeks were included in this dataset (denoted in red). A) SWNT$^+$ cells in the carotid artery (n=6, **p<0.01); B) SWNT$^+$ cells in the iliac artery (n=7, **p<0.01); C) SWNT$^+$ cells in the renal artery bifurcation (n=7, ***p<0.001); D) SWNT$^+$ cells in the bone marrow (n=7, p=0.4753). Statistical analyses were performed using an unpaired T test with Welch's Correction.

Taken together, these findings suggest that SWNT uptake is rare in all cells from non-vascular tissue, as well as in the non-MO/MΦ component of blood vessels. In contrast, significant enrichment is observed in the MO/MΦ population from each vascular tissue bed analyzed, highlighting their propensity to accumulate in the inflamed macrophages of the atheroprone vasculature (Manuscript Figure 3b). We thank the Reviewer for allowing us to clarify this important point.

4. Multiple flow results showed that SWNT-SHP1i was preferentially taken up by inflammatory monocytes and macrophages, either in the circulation or within plaques. What factors mediate the occurrence of this specific endocytosis?

Response: *We appreciate Reviewer #2's insightful question into an area of active investigation in our lab. From scRNA-sequencing and subsequent GO pathway analysis of isolated murine aortic atherosclerotic plaques, we found that Clathrin-mediated endocytosis was upregulated in the SWNT-SHP1i treated mice[4]. To determine if Clathrin-mediated endocytosis is a key mediator of SWNT uptake, we performed in vitro siRNA knockdown experiments of a critical component of this pathway, Clathrin heavy chain (CLTC). Our results did not demonstrate a significant reduction in SWNT uptake after knockdown of this factor compared to the scrsiRNA control (**Figure E**). These results suggest that Clathrin mediated endocytosis is unlikely to act as a major mediator of SWNT uptake, and that additional mechanisms and/or receptors are likely to be involved.*

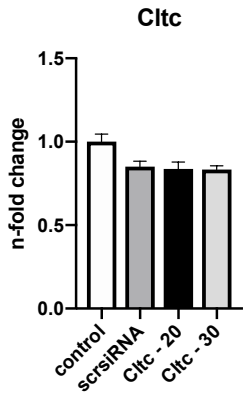

Figure E. SiRNA knockdown of Clathrin-dependent uptake component Cltc was performed *in vitro* and SWNT uptake was measured by flow cytometry analysis. Cltc 20 nM and 30 nM siRNA KD did not demonstrate a significant reduction compared to the scrsiRNA control group.

*To that end, we are currently pursuing additional putative mechanisms by which SWNTs are specifically taken up by MO/MΦ, including a receptor of interest, MARCO. MARCO is a key scavenger receptor, and a pattern recognition receptor thought to support complement-independent phagocytosis of foreign pathogens by macrophages. Initial flow cytometry experiments show that anti-MARCO inhibition results in a 60% reduction in SWNT uptake (**Figure F**). However, as was the case with Clathrin inhibition, uptake was not completely blocked, suggesting that macrophages likely specifically engulf our carbon nanotubes by other, yet-to-be-identified molecular mechanisms. These efforts are ongoing and will be reported in a future publication, once fully mapped.*

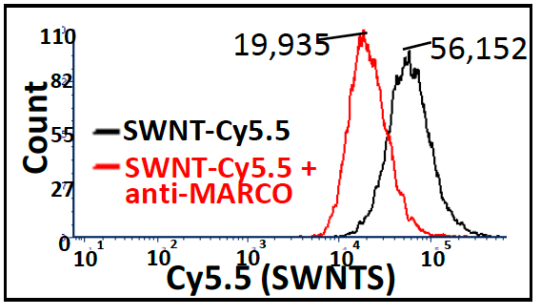

Figure F. Anti-MARCO antibody was incubated with inflammatory Mo/MΦ, then incubated with SWNTs. SWNT uptake was partially abrogated (~60%) by anti-MARCO, suggesting MARCO is one of (but not the only) the receptors enabling uptake.

5. The paper only shows blood safety during long-term treatment with different materials, but there are no blood samples from the diseased and healthy groups to serve as controls. Long-term drug treatment inevitably triggers chronic damage to the organism, and I believe it is necessary to observe various blood indices in healthy pigs to further ensure the long-term biosafety of SWNT-SHP1i.

***Response:** We thank the Reviewer for these thoughtful comments. As shown below (**Figure G**), we now provide clinical-grade laboratory results for the animals across the complete duration of the study. We found no significant differences between the SWNT and SWNT-SHP1i cohorts in their lab parameters at any timepoint, including the complete blood counts (RBC, Hgb, HCT, Platelets, WBC, neutrophil, lymphocyte, monocyte), their comprehensive metabolic panels (BUN, Cr, Albumin, AST, Alkaline Phosphatase), and their lipid panels (cholesterol, triglycerides, LDL).*

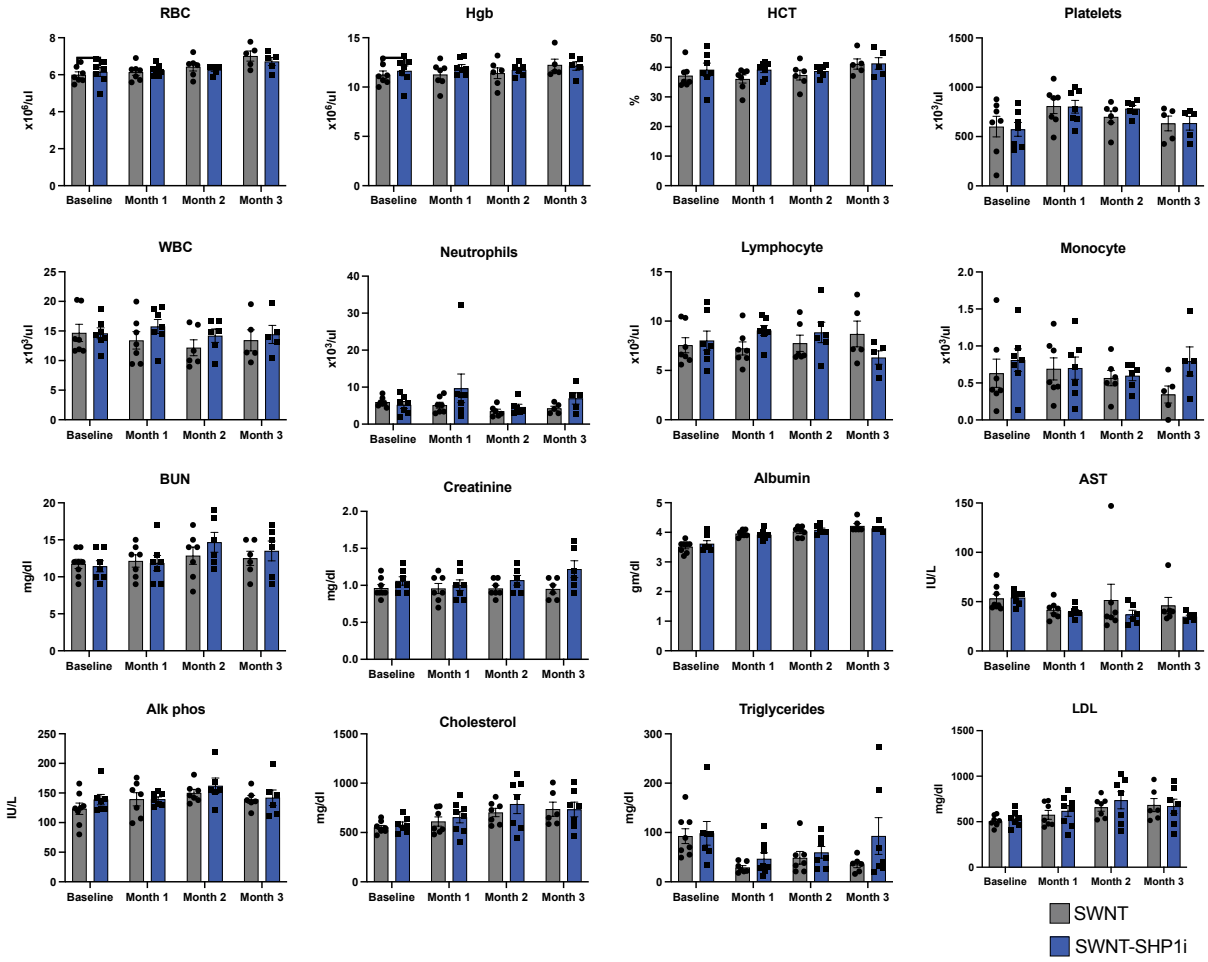

Figure G. Pigs treated with SWNT-SHP1i (n = 5-7/timepoint) do not develop anemia or thrombocytopenia. SWNT-SHP1i treatment was not significantly associated with differences in the CBC (RBC, Hgb, HCT, Platelets, WBC, neutrophil, lymphocyte, monocyte), CMP (BUN, Cr, Albumin, AST, Alkaline Phosphatase), or lipid panel (cholesterol, triglycerides, LDL) lab values compared to SWNT controls (n=5-7/timepoint). Statistical analysis was performed using an unpaired T test with Welch's Correction.

More specifically to the Reviewer's point, however, we agree that comparison must also be made to atheroprone animals that have not received SWNTs of any kind (with or without the SHP1 inhibitor). We now point out that SWNT therapy had almost no effect on any laboratory parameter of clinical interest compared to pre-treatment baseline levels and note that the vast majority of lab values remained within the reference range through the course of the study. The two exceptions to this included platelet count and alkaline phosphatase levels (Figure G). Specifically, platelets were elevated in both the SWNT and SWNT-SHP1i LDLR$^{-/-}$ cohorts even at baseline (before SWNT administration) and at every subsequent time point (Months 1-3).This finding is possibly reflective of the role of platelets as an acute phase reactant that can be elevated in settings of chronic inflammation such as those induced by severe dyslipidemia induced by LDLR knockout and hypercholesterolemia[5]. The stability of these values during the course of the study reduced our suspicion that the nanotherapy was contributing to the abnormal laboratory finding. Similarly, alkaline phosphatase (Alk Phos) levels, which are known to be increased secondary to elevated CVD risk[6], were above the reference range at baseline in the SWNT-SHP1i cohort and remained elevated in both cohorts at months 1-3. Taken together, we believe our findings from the

comparison of baseline and monthly labs supports the safety and tolerability of this new translational therapy.

6. Does the loading rate of SHP1i change in mass-produced SWNT-SHP1i?

Response: *We thank the Reviewer for this question. The loading rate of SHP1i on SWNTs can be engineered to desired levels, independent of the scale of production. Therefore, the loading rates of SHP1i in mass-produced SWNT-SHP1i can be tuned to the same levels as on our previous small batch SWNTs using chemistry and stoichiometry. Hence, for a given batch, small or mass-produced, the approximate number of SHP1i per SWNT can be chosen and the SWNT-SHP1i produced, as was performed in this case.*

Reviewer #3 (Remarks to the Author):

Major Comments

The authors have previously reported that reactivating efferocytosis, the process by which macrophages phagocytose inflamed cells, holds promise for translational research in atherosclerotic cardiovascular disease. They have shown that blocking CD47 can reduce plaque burden by enhancing the clearance of apoptotic vascular tissue. However, it's important to note that systemic CD47 blocking can lead to anemia, necessitating clinical attention.

In this study, the authors introduce the concept of a "Trojan horse" macrophage-specific nanotherapy and test it in an LDLR-/- porcine model of atherosclerosis. Their aim is to determine whether this approach justifies further investigation in human clinical trials. Notably, their research extends their previous work conducted in a murine model of atherosclerosis, demonstrating the scalability and translational potential of their findings. In the early stages of the disease, their pro-efferocytic nanotherapy effectively reduces the accumulation of apoptotic cells and induces anti-inflammatory changes within the plaque.

1. The FACS analysis results to support that SWNTs are preferentially taken up by monocytes in the circulation lack rigor. It's important to include an overall percentage of all immune cells detected, along with the frequency of $SWNT^+$ and $SWNT^-$ cells in each population. Additionally, the spectral unmixing model should be validated with compensation controls, and spectral fluorescence signature data of stained and unstained samples should be provided.

Response: *We appreciate the Reviewer's comments and fully concur. We have now performed several additional experiments to clarify how our flow cytometry analyses were performed, and to specifically address each of the Reviewer's questions.*

*First, we now provide what we believe to be a more clearly depicted gating strategy, highlighting how we identified each cell type in the circulation (**Figure H**). We also now include compensation controls and spectral fluorescence signatures of unstained and stained samples for comparison (**Figures I, J**), as requested.*

Gating strategy:

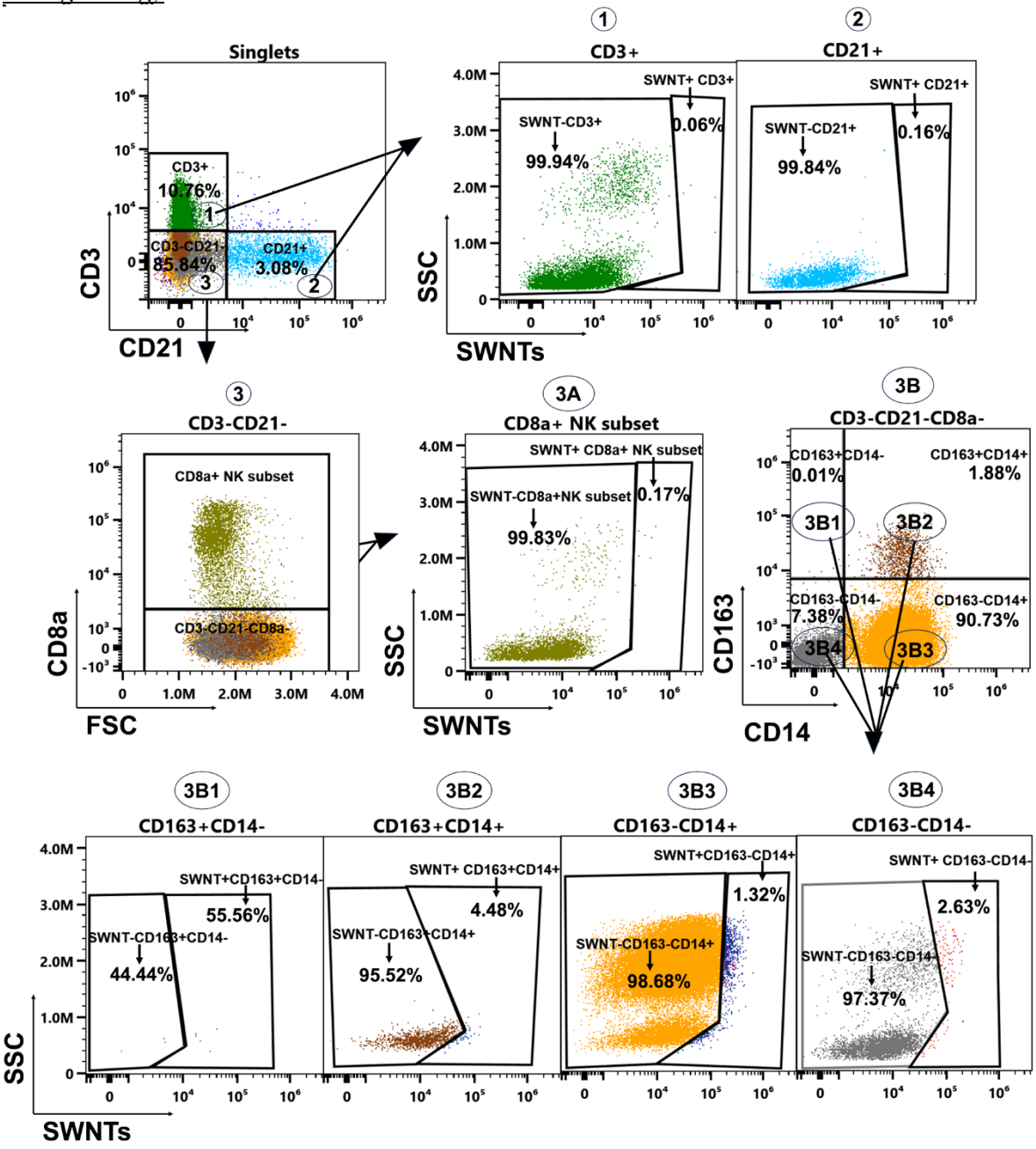

Figure H: Gating strategy and representative dot plots of blood samples from a SWNT-SHP1i treated pig (7 days post-treatment).

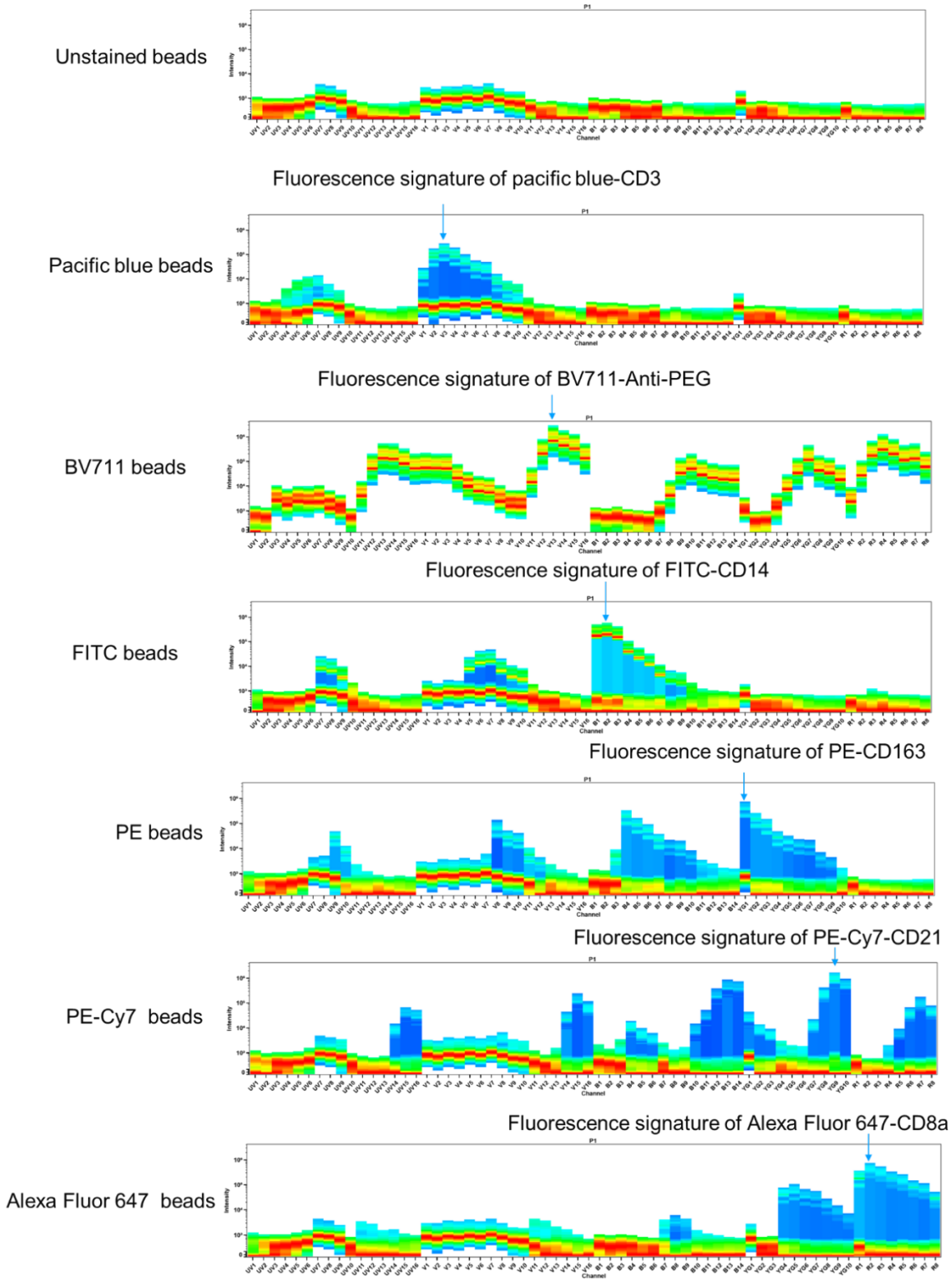

Figure I. Spectral signatures of the compensation beads used as single stained controls in our Cytek Aurora flow cytometer. Each fluorophore shows a peak fluorescence in a specific channel.

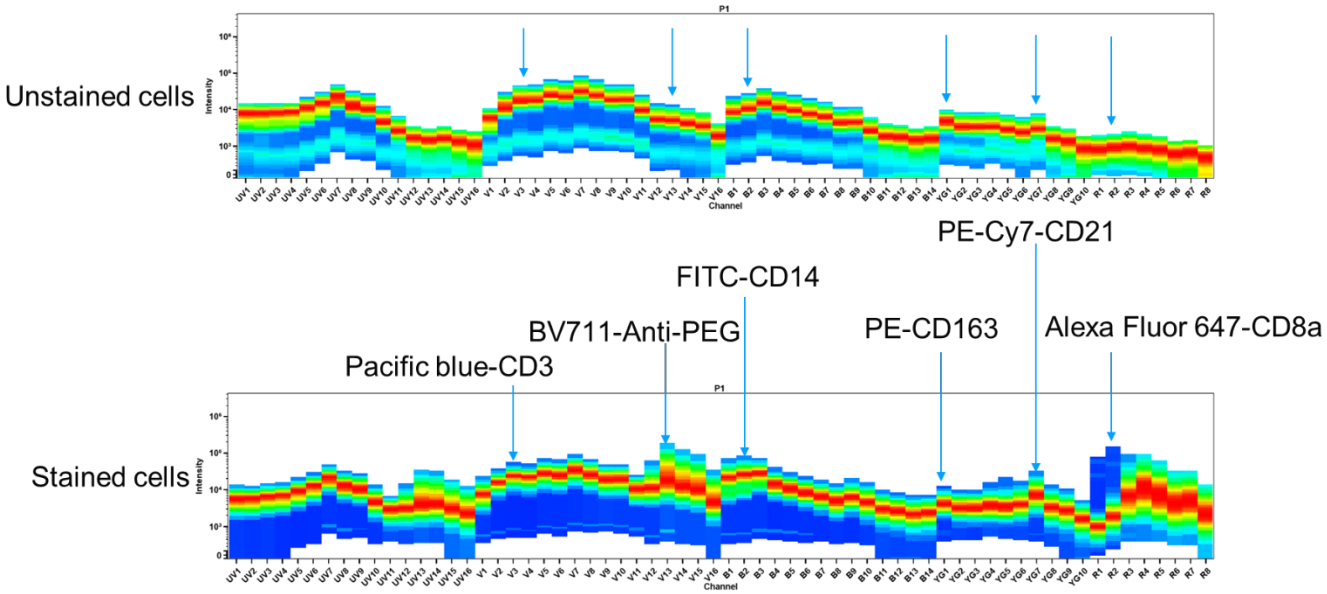

Figure J. Fluorescence spectra of unstained (top) and stained (bottom) cells showing fluorescence related to different fluorophores used in cell staining. Each fluorophore shows peak fluorescence in a specific channel of the Cytek Aurora flow cytometer.

*Next, we calculated the percentage of each cell type in the circulation of our animals at the terminal endpoint of the study, after 3 months of high fat diet and treatments. SWNT-treated pigs showed an average of 33.3% T cells, 9.5% B cells, 6.9% CD8a$^+$NK cells, and a 38.1% MO/MΦ population, along with an 11.9% 'other' cell type subpopulation 2-weeks after completion of the therapy and immediately prior to sacrifice (**Figure K**). SWNT-SHP1i treated pigs had a similar distribution of immune cell types at this timepoint (**Figure K**).*

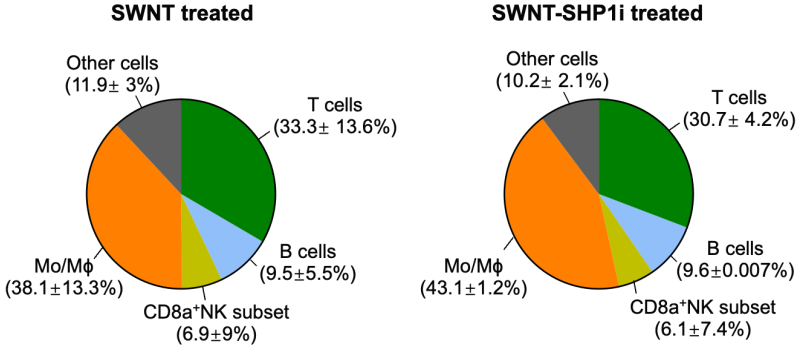

Figure K. Percent of each immune cell type identified in the blood of 12 week treated pigs (analyses performed 2 weeks post treatment, n=2 per group).

*We then analyzed each circulating immune cell subtype according to the proportion of SWNT positivity. SWNT uptake was largely restricted to MO/MΦ, including the CD163$^+$/CD14$^-$ population (**Figure L**).*

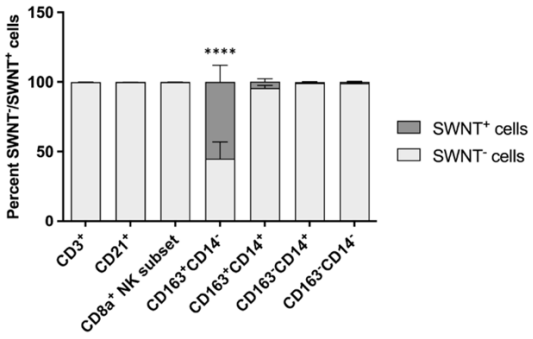

Figure L. Average proportion of SWNT⁻ and SWNT⁺ immune cell types including B, T, and NK cells, as well as MO/MΦ across SWNT/SWNT-SHP1i treated pigs. ****P<0.0001 CD163⁺CD14⁻ cells versus other cell types. Statistical testing was performed using a one-way ANOVA.

*Finally, to confirm that SWNT uptake in blood corresponds to uptake by MO/MΦ in inflamed blood vessels, we generated single cell suspensions of atherosclerotic vessels and performed flow cytometric analyses. We then compared those results to those from non-vascular tissue beds. We found that SWNTs are selectively enriched in certain phagocytic cells in the atheroprone carotid arteries, iliac arteries, and the renal artery bifurcation. SWNTs are not generally endocytosed by macrophages from non-inflamed organs (e.g. bone marrow), or non-immune cells in any of the organs evaluated (**Figure C**).*

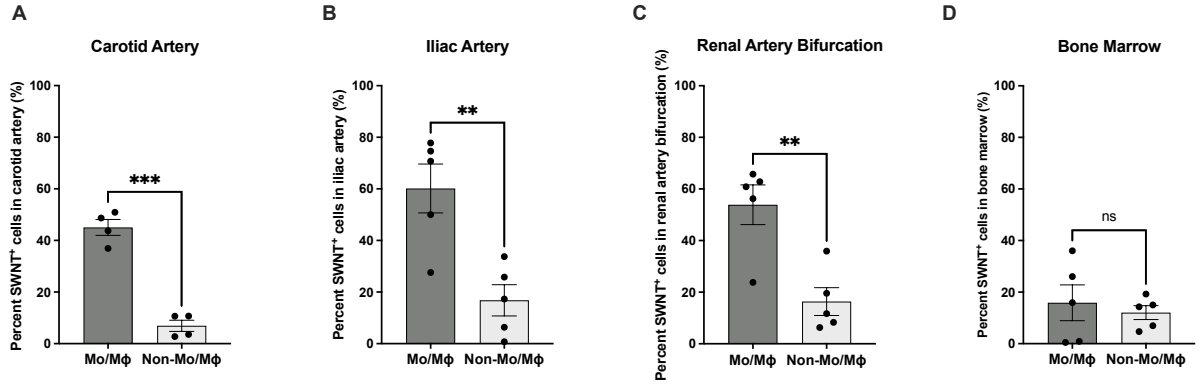

Figure C. SWNTs/SWNT-SHP1i were selectively taken up by the MO/MΦ population of vascular tissues containing atherosclerotic lesions as compared to similar populations from the bone marrow. A) SWNT⁺ cells in the carotid artery (n=4, ***p=0.0001); B) SWNT⁺ cells in the iliac artery (n=5, **p<0.01); C) SWNT⁺ cells in the renal artery bifurcation (n=5, **p<0.01); D) SWNT⁺ cells in the bone marrow (n=5, p=0.6314). Statistical analyses were performed using an unpaired T test with Welch's Correction.

2. In Figure 2, there are concerns about legibility and clarity:
- The axis labels need adjustment for improved readability.

- ***Response:*** *We agree with the Reviewer and have increased the font size to improve readability and also re-arranged the figure. We furthermore included SWNT⁻ gates in the figure and the bar diagram now represents the data for both SWNT⁻ and SWNT⁺ cells. Additionally, we now combined the data for both SWNT and SWNT-SHP1i treated pigs, considering that SHP1i loading on SWNTs is not expected to significantly change the uptake of SWNTs.*

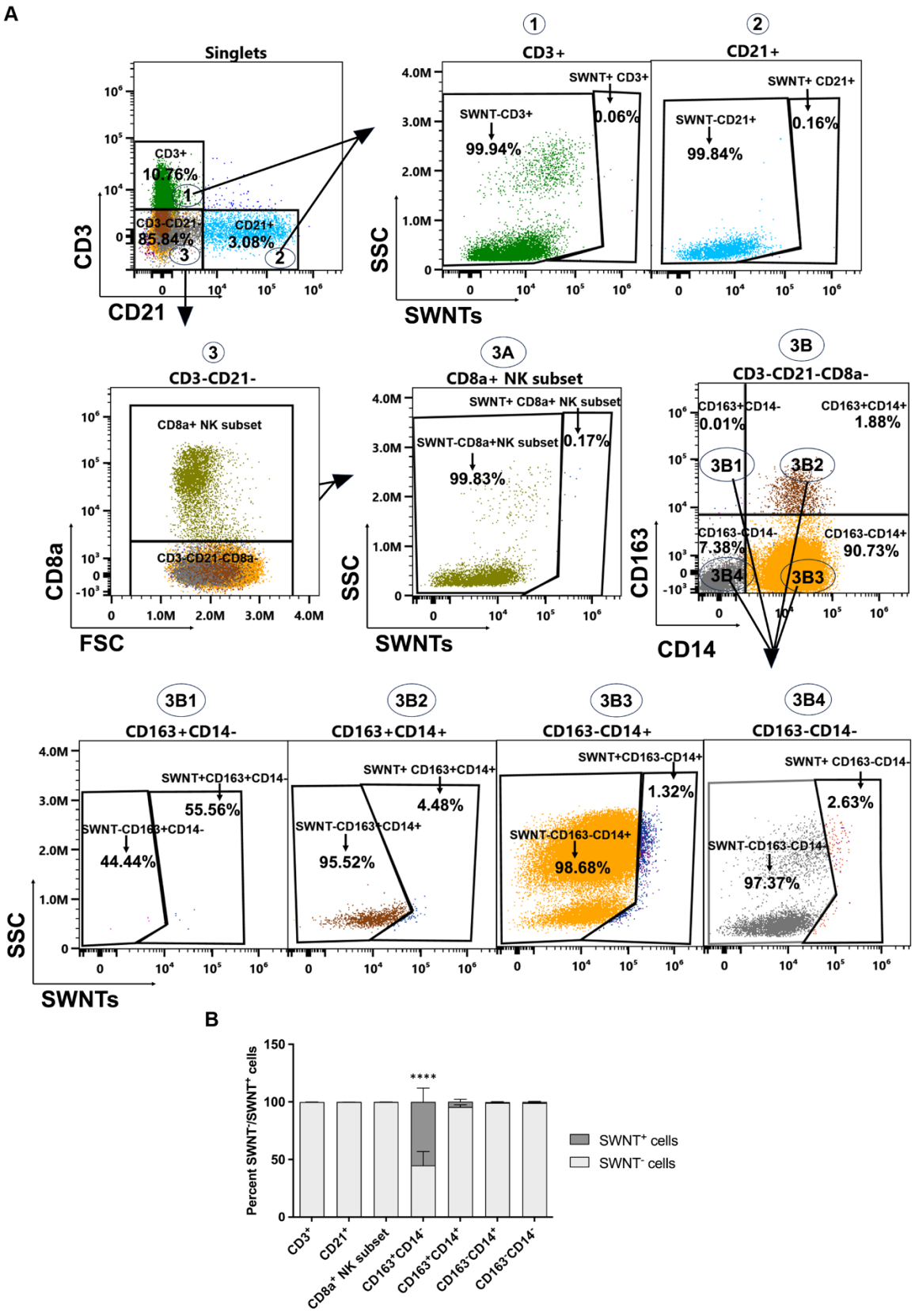

Figure 2: SWNTs are preferentially taken up by monocytes in the circulation.

- The directionality of the populations of interest, including the singlets suggesting the $CD21^+$ and $CD3^-$ $CD21^-$ populations (NK population), should be clarified for better understanding.

Response: *We apologize for the confusion and appreciate the opportunity to clarify our methodological approach. After excluding doublets, we gated all singlets to identify different immune cell populations. $CD3^+$ and $CD21^+$ cells, which represent porcine T cells and B cells, respectively, were gated in the singlet population and the remaining cells (excluding $CD3^+$ and $CD21^+$ cells) were named $CD3^-CD21^-$ cells. Thereafter, the $CD3^-CD21^-$ cells were gated for the $CD8a^+$ NK subset and the remaining cells labeled $CD3^-CD21^-CD8a^-$ were further gated for different subsets of monocytes. A quadrant gate was applied on $CD3^-CD21^-CD8a^-$ cells based on fluorescence from CD163 and CD14 antibodies. $CD163^+CD14^-$, $CD163^+CD14^+$, and $CD163^-CD14^+$ cells were considered different types of monocyte populations, while $CD163^-CD14^-$ cells were considered other cell types, excluding all the immune cell types described above. We have now added more arrows to specify the parent population of the monocyte subtypes and further explained these details in the revised methods section.*

- It would be beneficial to include data on the overall percentage of major immune cell types in the model, especially the monocyte percentage and T cell percentages before and after SWNT uptake.

Response: *We appreciate the comment and gated the percentage of immune cell types before and after SWNT/SWNT-SHP1i treatment in pig whole blood. We found no differences before and two weeks after injection. These data suggest that injection of SWNT/SWNT-SHP1i did not induce changes in the immune cell content of the blood (**Figure M**).*

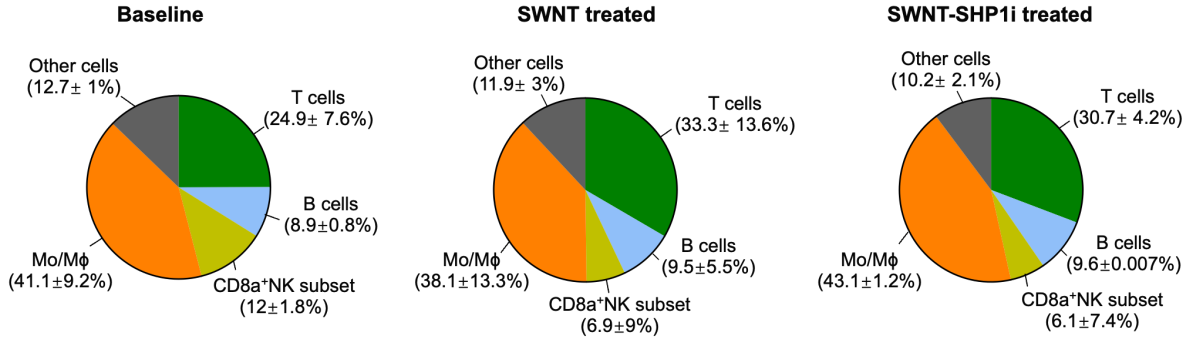

Figure M. Pie charts of leukocyte percentages before (n=2) and after SWNT/SWNT-SHP1i treatment (n=2 per group) in whole blood from pigs. One-way ANOVA analysis showed no significant differences between different cell types. Analysis was performed on blood samples received 2 weeks after the last treatment.

- Given that flow cytometry was performed with whole blood samples, the percentage of neutrophils and their potential role in nanoparticle uptake should be discussed.

Response: *We appreciate the Reviewer's comment regarding neutrophils, particularly given their phagocytic nature. We previously had directly addressed this question in mouse models and found very low neutrophil uptake of SWNTs when injected in vivo (reproduced in **Figure N** below)*[7].

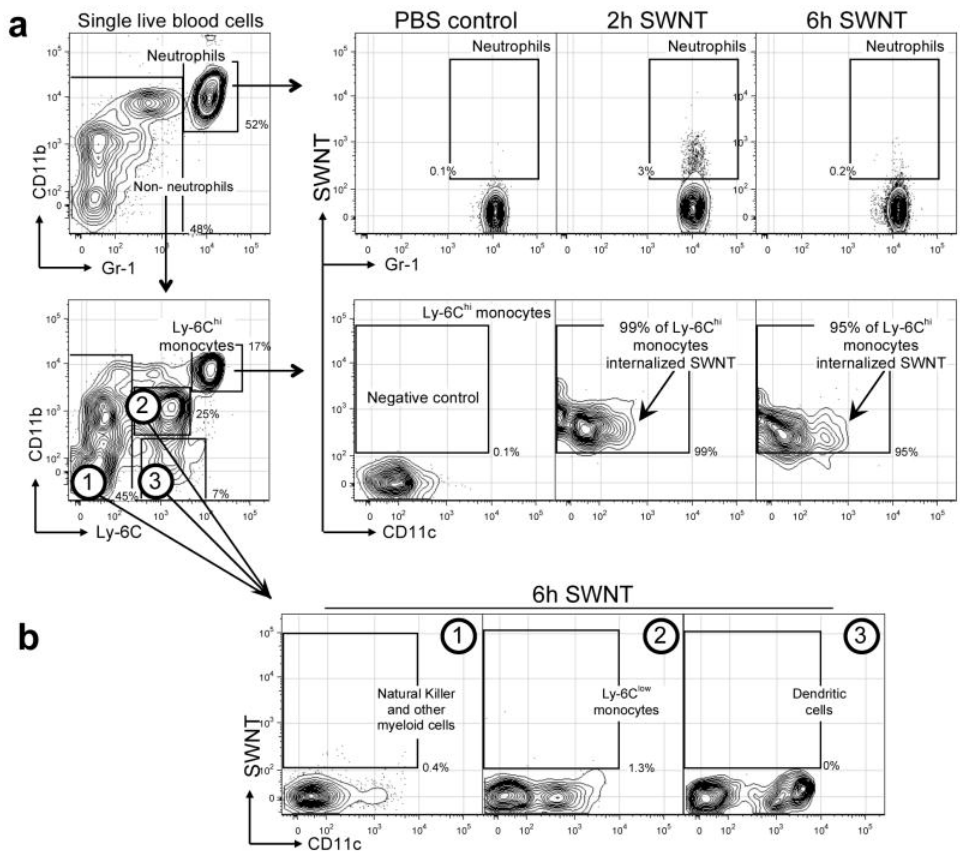

Figure N. From *Nat Nanotechnol*. 2014 Jun; 9(6): 481–487[7]. Neutrophil uptake is shown along the top right. Flow cytometry plots reveal minimal uptake (0.2-3.0%) at either timepoint.

*To extend this work into our pig model, we used an indirect flow cytometric method given that we did not include a neutrophil-specific marker in the original panel of flow antibodies. We stained whole blood cells with a mono/granulocyte marker (SWC3) in one panel and CD163 and CD14 markers for Mo/MΦ in another panel (**Figure O**). We estimated neutrophil uptake by calculating the percent SWNT$^+$ monocytes + granulocytes (Figure O panel 1) and then deducted the percent of MO/MΦ (Figure O panel 2) from this population to quantify the percentage of granulocytes taking up SWNTs. As shown below, only ~1.6% of putative neutrophils take up SWNTs in the circulation (**Figure O**), in keeping with our published mouse findings above.*

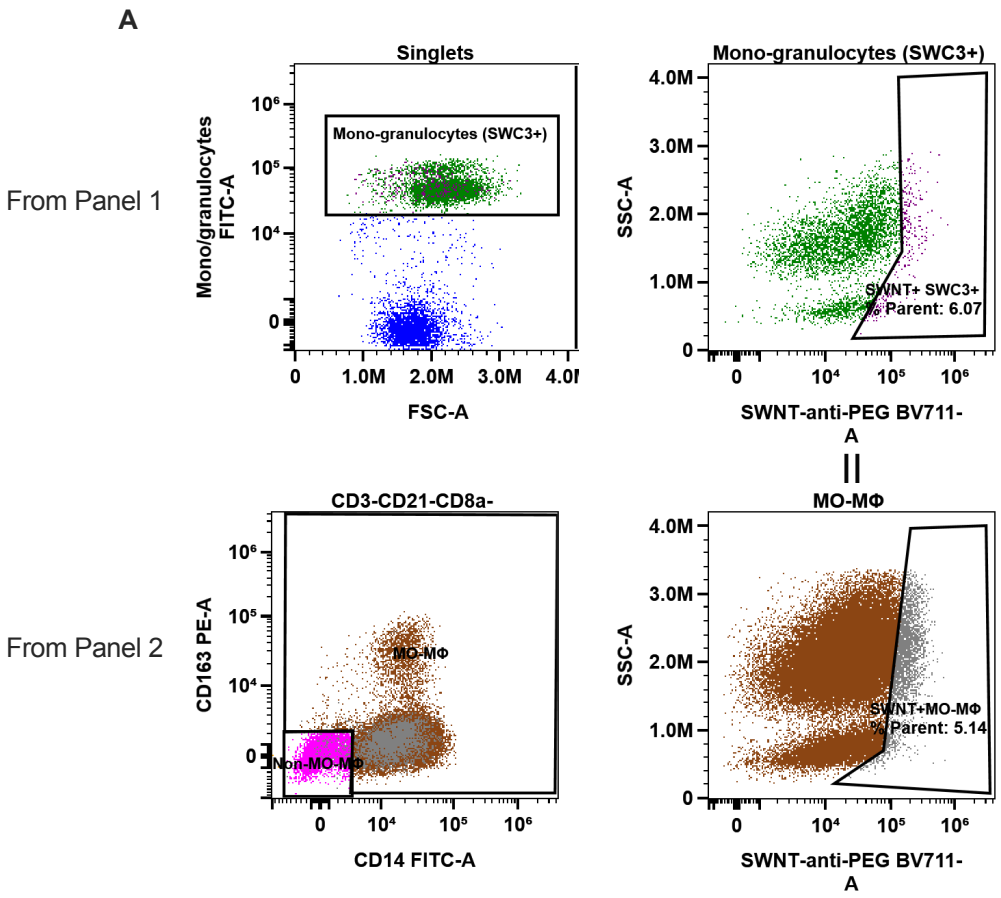

B Bar diagram showing the average value of I minus II

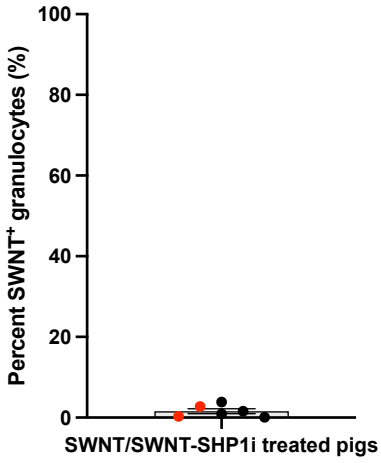

Figure O: Estimation of percent SWNT$^+$ granulocytes in pig blood (n=6). A) Representative gating strategy for estimating SWNT$^+$ granulocytes. B) Bar diagram showing average percent SWNT$^+$ granulocytes. Red dots indicate the data points from the small cohort treated for two weeks only; black dots represent treatment for 12 weeks.

*These flow-based results were then compared with clinical laboratory results from our Complete Blood Counts (CBCs) with Differential panels. As shown below, in both SWNT and SWNT-SHP1i cohorts, the neutrophil population does not change between the pre-treatment baseline and month 3 of treatment (**Figure P**), further supporting previously published findings as well as the flow cytometry analysis (**Figure O**). We thank the Reviewer for the opportunity to clarify this point.*

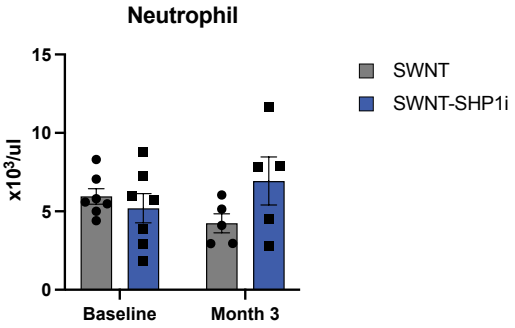

Figure P. Neutrophil count is not significantly different in SWNT (n=5-7/timepoint) versus SWNT-SHP1i (n=5-7/timepoint) treated cohorts at baseline and 3 months. No differences were noted in the SWNT-SHP1i cohort compared to pre-treatment baseline levels. Statistical analysis was performed using an unpaired T test with Welch's Correction. Statistical analysis comparing timepoints was performed using a one-way ANOVA.

3. CBC should include the leukocyte count results, which are part of the standard test.

***Response:** We appreciate Reviewer #3's suggestion to include the leukocyte count, which we have now incorporated into Figure 5. We also now include additional lab parameters from the CBC with differential (**Figure Q**). The average WBC count for SWNT and SWNT-SHP1i cohorts was within normal limits, with no significant difference between the two groups at baseline or the 3 month timepoint.*

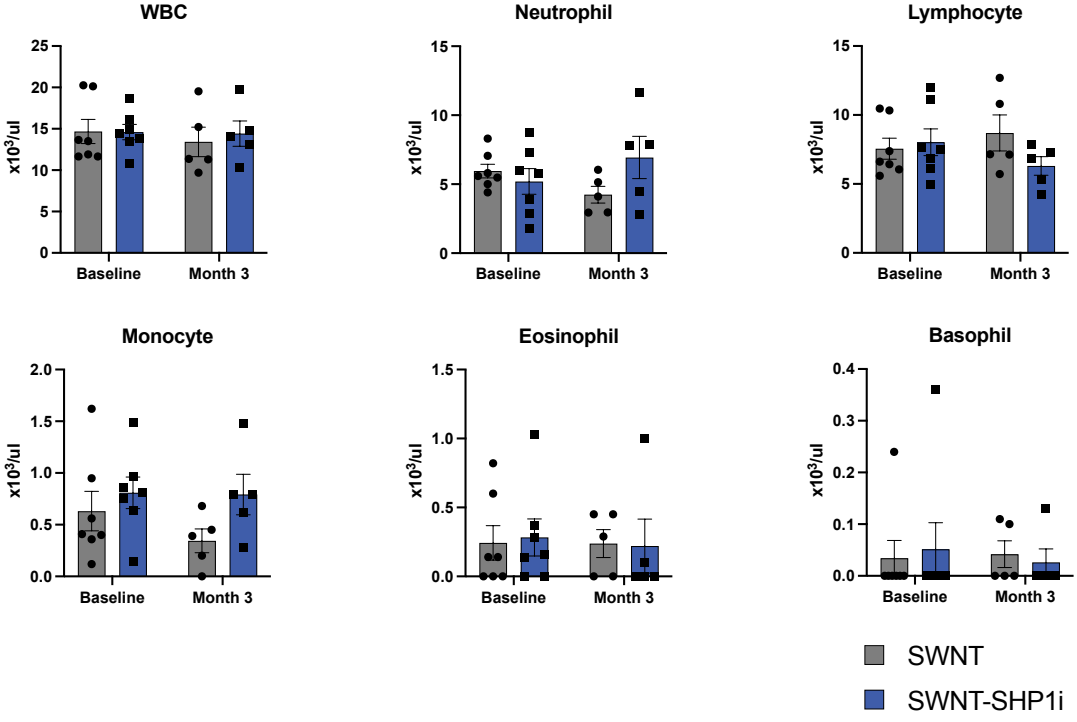

Figure Q. SWNT-SHP1i (n=5-7/timepoint) treatment was not significantly associated with differences in WBC, neutrophil, lymphocyte, monocyte, eosinophil, or basophil lab values compared to SWNT controls (n=5-7/timepoint). No differences were noted in the SWNT-SHP1i cohort compared to pre-treatment baseline levels. Statistical analysis between SWNT and SWNT-SHP1i was performed using an unpaired T test with Welch's Correction. Statistical analysis comparing timepoints was performed using a one-way ANOVA.

4. The authors should provide clearer information about which animals were used for each experiment.

Response: *We apologize for the confusion and appreciate the opportunity to clarify which animals were used for each experiment. In the methods section, we now specify that the ORO, IBA-1, and TUNEL staining were performed on all available vascular tissue from SWNT and SWNT-SHP1i treated pigs. We also point out that due to limited availability of animal transport services and scanner access at the University of Iowa, 5 pigs from each treatment cohort were randomly selected to undergo PET/CT imaging at 12 weeks. Also, we now specify that flow cytometry studies were done on blood and tissues obtained from SWNT treated and SWNT-SHIP1i treated pigs. Furthermore, all available laboratory values from each cohort were included in the analysis.*

5. In Figure 3:
- The gating strategy, particularly the shape of the gating shown in the representative figure, is not clear. An unstained control should be included to justify the gating.

Response: *We thank the Reviewer for helping us clarify our strategy to the readers. In the revised manuscript, we now include our unstained and fluorescence minus one (FMO) controls for anti-PEG antibody used to justify our gating. Gating was performed using an FMO control approach, in which every antibody except anti-PEG was added, as shown below. Moreover, we simplified the shapes of the gates (**Figure R**; Manuscript **Supplemental Figure 3**). We also now provide pooled uptake data of SWNT and SWNT-SHP1i treated pigs. Please also see the compensation controls provided in response to Query 1, above **(Figure I-J)**.*

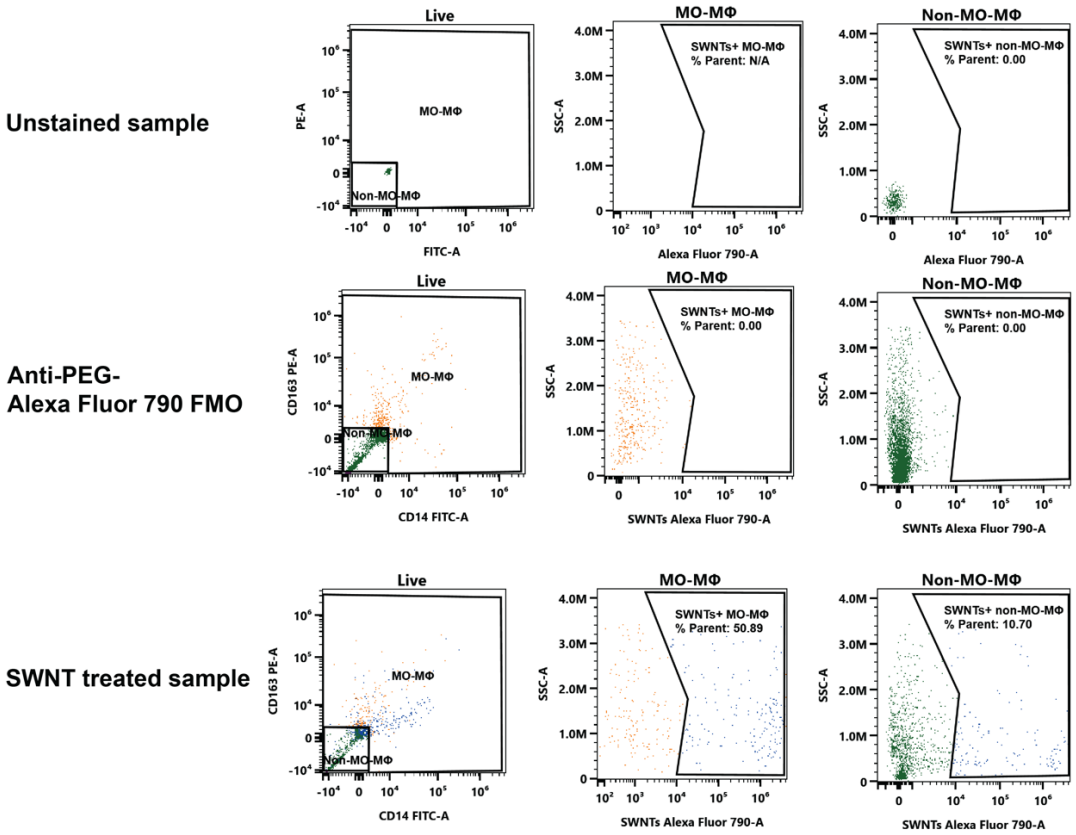

Figure R. Flow cytometry gating strategy for analysis of pig carotid arteries. Representative dot plots of unstained, anti-PEG-Alexa Fluor 790 FMO, and SWNT treated pig samples are displayed.

- Figure 3d: It should be clarified whether the ORO histology was performed in mice or pigs. Additionally, the scale bar is not visible.

Response: *We appreciate Reviewer #3's suggestion and have corrected the figure legend to clarify that ORO histology was performed in pigs. We also increased the font on the scale bar for improved readability (**Figure 3**).*

- The scale bar is missing in most representative figures.

Response: *Thank you for this suggestion. Similar to the ORO images, we have increased the scale bar font for the IBA1 and TUNEL images to improve readability (**Figure 3**).*

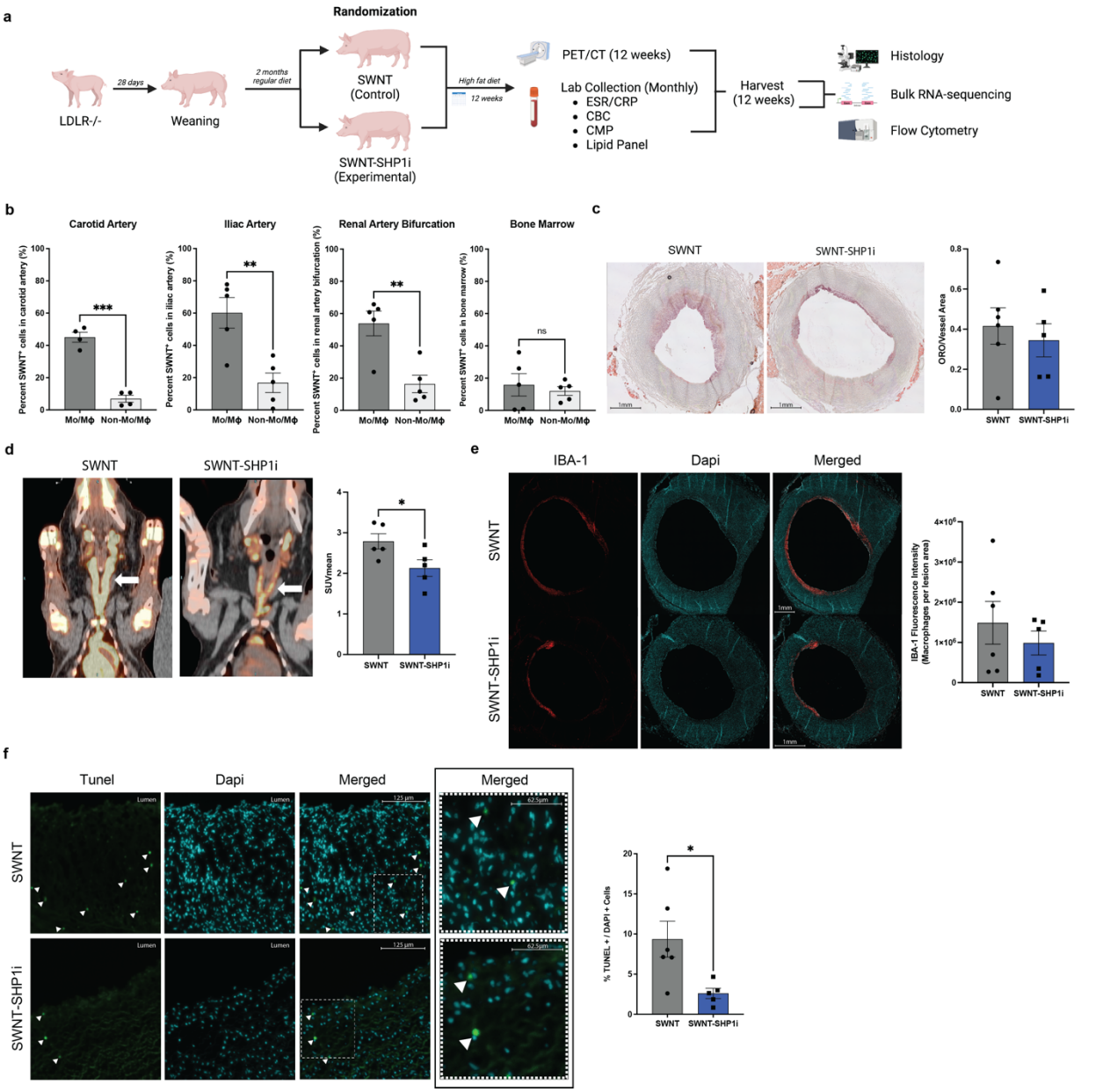

Figure 3. SWNTs accumulate in atherosclerotic plaque and SHP1 inhibition reduces both vascular inflammation and apoptotic cell accumulation in transgenic atherosclerotic pigs, *in vivo*.

6. In Figure 3c, bar plots should include dots. It is concerning that only two pigs per group were analyzed, raising statistical concerns.

Response: *We thank the Reviewer for this suggestion. In the revised manuscript, we have combined data from the SWNT and SWNT-SHP1i treated animals, and now provide bar plots which have been revised to include dots (Figure 3b). This pooled uptake data shows enrichment of SWNTs within the MO/MΦ population within the atherosclerotic carotid artery. To validate and extend these results, we also now provide a similar analysis on atherosclerotic iliac vessels as well as at the renal artery bifurcation, which confirms similar patterns in additional vascular beds. Importantly, no such enrichment was observed in a non-vascular tissue bed, further supporting the concept that SWNT enrichment is restricted to inflamed/atheroprone vessels (**Figure C**; **manuscript Figure 3b**).*

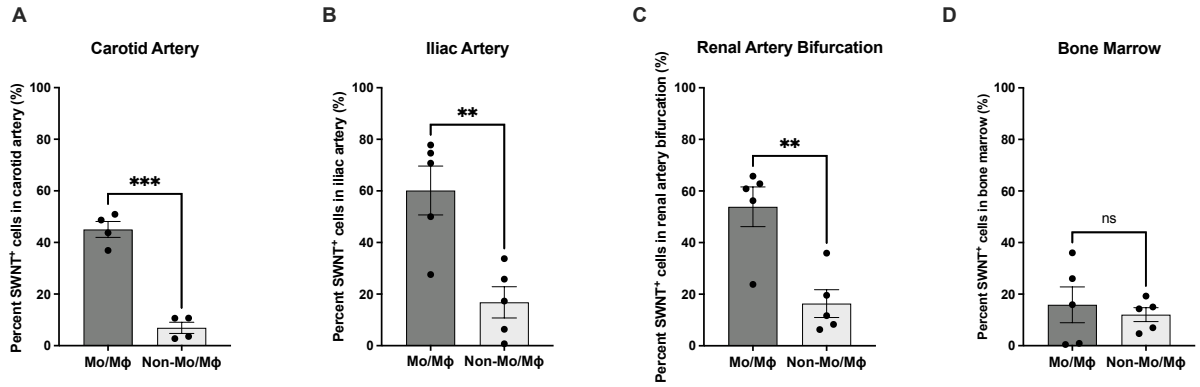

Figure C. SWNTs/SWNT-SHP1i were selectively taken up by the MO/MΦ population of vascular tissues containing atherosclerotic plaques as compared to a similar population from the bone marrow. A) SWNT$^+$ cells in the carotid artery (n=4, ***p=0.0001); B) SWNT$^+$ cells in the iliac artery (n=5, **p<0.01); C) SWNT$^+$ cells in the renal artery bifurcation (n=5, **p<0.01); D) SWNT$^+$ cells in the bone marrow (n=5, p=0.6314). Statistical analyses were performed using an unpaired T test with Welch's Correction.

Finally, per the request of another Reviewer, we have included new data from a small cohort of animals treated with a short course (2 weeks) of Cy5.5 fluorophore-labeled nanoparticles to confirm the preceding flow cytometry results. As shown below in ***Figure D****, a consistent pattern of enrichment continues to be observed in this combined analysis (which is shown as 'Reviewer-only', given the different time courses used in each experiment [2 weeks vs 3 months]).*

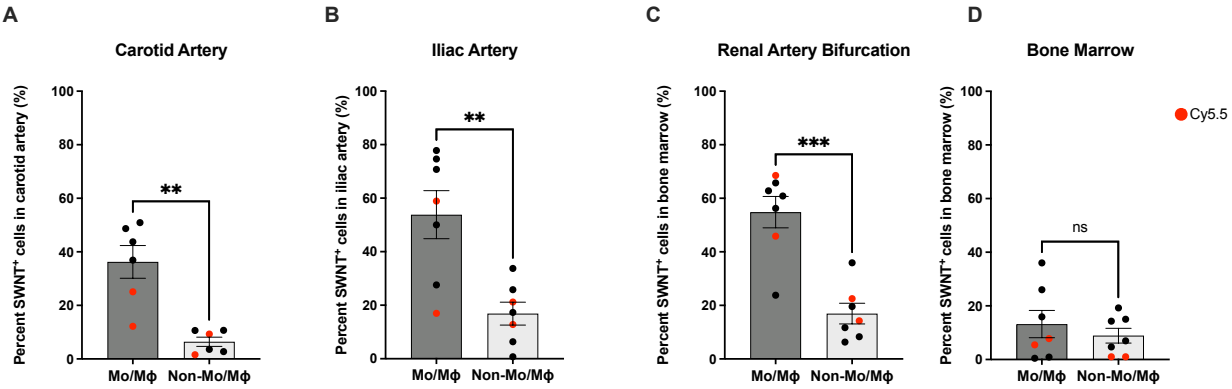

Figure D. SWNTs/SWNT-SHP1i were selectively taken up by the MO/MΦ population of vascular tissues containing atherosclerotic plaques as compared to a similar population of cells from the bone marrow. Pigs treated with Cy5.5 tagged-SWNT (n=1) or SWNT-SHP1i (n=1) for two weeks were included in this dataset (indicated in red). A) SWNT$^+$ cells in the carotid artery (n=6, **p<0.01); B) SWNT$^+$ cells in the iliac artery (n=7, p<0.01); C) SWNT$^+$ cells in the renal artery bifurcation (n=7, ***p<0.001); D) SWNT$^+$ cells in the bone marrow (n=7, p=0.4753). Statistical analyses were performed using an unpaired T test with Welch's Correction.**

We thank the Reviewer for the opportunity to present these additional analyses and clarify the pattern of enrichment in phagocytic cells within the atheroprone blood vessel.

7. Figure 4's RNA seq analysis lacks attention to detail. The integration methods for RNA seq are not described, and the volcano plot does not allow proper visualization of genes. The Venn diagram mentions that >40 genes overlap between species, but only 10 are listed.

Response: *We appreciate the opportunity to address the Reviewer's comments regarding our RNA-seq analyses. In the revised Methods section, we attempt to clarify our approach, and provide a description of the revised analyses (which separately present the pig-only and integrated results). Briefly, we now write, "Significant DEGs (p adj. <0.05) from the pig bulk RNA-Seq were inputted into the gene ontology (GO) knowledgebase to identify functions and pathways associated with the DEGs. In order to integrate the pig bulk RNA-seq data with the previously published murine single-cell RNA-seq (Flores et al 2020 Supplemental Table 1[4]), cluster 1&4 DEGs (representing the macrophage and monocyte subpopulations, respectively) were filtered to create a separate table. Shared DEGs were identified using excel to highlight duplicate gene names included in both the pig bulk RNA-seq and mouse scRNA-seq (clusters 1&4) lists. DEGs were then inputted into the PANTHER Pathway for GO term enrichment analysis to allow for the identification of conserved pathways in both porcine and murine models."*

Additionally, we adapted ***Manuscript Figure 4*** *(see below) so that it includes all 35 overlapping DEGs, and - for completeness - we now also provide a separate analysis restricted solely to the pig bulk RNA-sequencing DEGs and GO biological process pathways (see new* ***Supplemental Table 1*** *and* ***Supplemental Figure 5****). We hope this addresses the Reviewer's question, but please do not hesitate to let us know if additional analyses would be viewed as informative.*

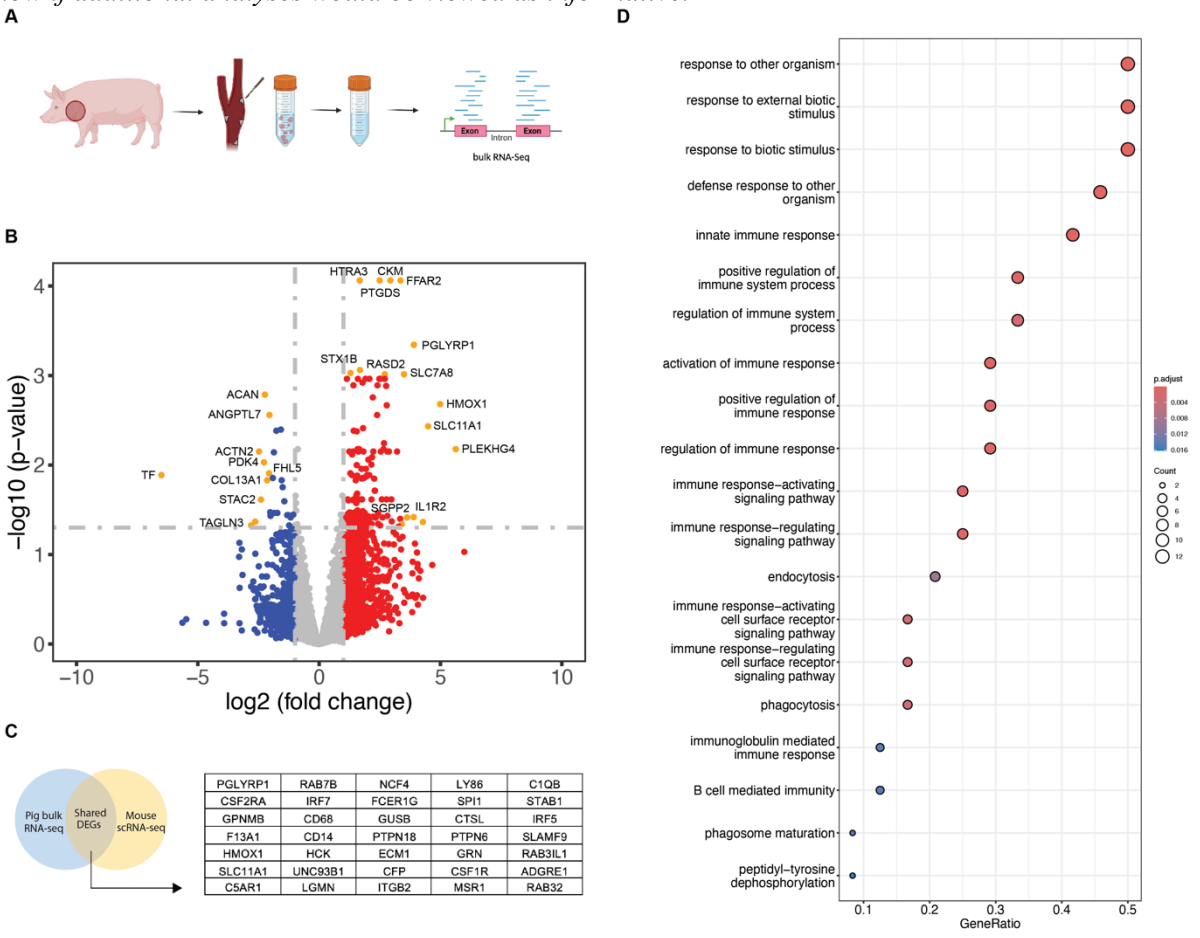

Figure 4. Pro-efferocytic therapies induce favorable immunological gene expression changes across species.

8. In Figure 4, the GO enrichment and pathway analysis should include pathways related to efferocytosis. The GO terms for heme metabolism and alterations in neutrophil activation should be addressed. The presence of several genes related to scavenger receptors, solute carrier transporters, and immune cell activation should also be discussed.

Response: *We appreciate the Reviewer's suggestions and the opportunity to address these key discussion points. Interestingly, the term 'efferocytosis' is not annotated in the GO library terms, thus explaining its absence from the list. During revision, we updated our GO enrichment and pathway analysis of overlapping DEGs between the pig bulk RNA-sequencing and the mouse MO/MΦ scRNA-sequencing data using the newly released PANTHER Overrepresentation Test (Released 02/26/2024). These analyses highlight a number of pathways related to response to external biotic stimulus, immune system regulation, endocytosis, and phagocytosis (See* ***Figure 4d*** *above). We have now added commentary about the most highly upregulated DEGs as well as GO enrichment and pathway analysis findings to our revised discussion, highlighting how our therapy appears to consistently trigger immune processes relevant to the identification and removal of danger signals across species.*

Minor Comments

1. In Figure 1, the legend should explain the meaning of T% (Fig. 1c).

Response: *We apologize for this omission and have revised the y axis legend to specify that "T%" stands for "Transmittance %". We have explained in the Figure legend that this readout refers to the FT-IR spectroscopy of SWNT and SWNT-Cy5.5-SHP1i.*

C

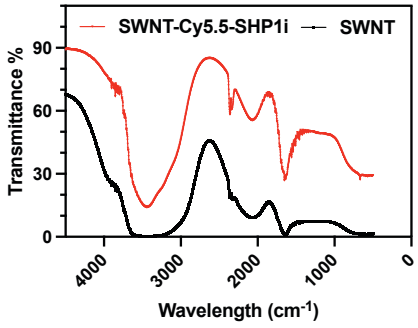

Reviewer #4 (Remarks to the Author):

In the submitted manuscript, Bamezai et al. upscale and test a nanoparticle-based experimental therapy to block CD47-induced signaling in macrophages in LDL receptor knockout minipigs. In a previous elegant study in mice, the group showed that these nanoparticles could reduce atherosclerosis, stimulate phagocytosis of apoptotic remnants, and reduce necrotic core size. The effort to translate this promising approach toward clinical studies by testing it in a large animal model is laudable. Unfortunately, however, the authors do not obtain clear positive results with respect to the efficient loading of monocytes in blood or its effects on atherosclerosis, which is only studied at a very early stage. Furthermore, 3 out of 14 pigs died of which 2 may have been nanoparticle-related deaths.

Major issues
1. Figure 1. It is concluded in the text that 78%/42% CD163+CD14- are positive for the nanoparticles, but these are fractions of rare cell populations. For the much more abundant CD14+ CD163- population, the fraction is only a few percent, raising questions about whether this is enough to have any impact. The fraction is much less than in the authors' previous paper in mice (ref 11). If the reason is a problem in detection, there may be no way around doing at least some fluorophore-coupled studies. It would also be helpful to discuss how these monocyte subgroups compare to those of the mouse studies.

***Response**: We thank the Reviewer for these insightful comments and suggestions. As suggested, we have now treated two additional animals with a short course of SWNT or SWNT-SHP1i conjugated with Cy5.5. Because of the extreme cost of the fluorescent probe (additional $9,520/dose/pig at the quantity needed to treat full-sized animals, in addition to the cost of the SWNTs, themselves), we injected each animal with 2 weekly doses of fluorophore-conjugated nanoparticles prior to sacrifice. Similar to the original experiments performed with unlabeled SWNTs, we found that $CD163^+CD14^-$ cells continued to show the highest percentage of Cy5.5 positivity (6 days after the final injection), and that the data were consistent with that obtained when defining SWNT uptake based on anti-PEG staining in the same animals. The absolute difference between the percent of $SWNT^-$ cells in the Cy5.5 (n=2) and anti-PEG analysis (n=2) was: $CD3^+$ (0.01%), $CD21^+$ (0.07%), $CD8a^+$ NK subset (0.75%), $CD163^+CD14^-$ (3.57%), $CD163^+CD14^+$ (1.65%), $CD163^-CD14^+$ (2.34%), $CD163^-CD14^-$ (0.06%). Similarly, the absolute difference between the percent of $SWNT^+$ cells in the Cy5.5 (n=2) and anti-PEG analysis (n=2) was: $CD3^+$ (0.00%), $CD21^+$ (0.09%), $CD8a^+$ NK subset (0.76%), $CD163^+CD14^-$ (3.57%), $CD163^+CD14^+$ (1.84%), $CD163^-CD14^+$ (2.25%), $CD163^-CD14^-$ (0.01%). Together, these important new data confirm that defining SWNT positivity based on the presence of PEG staining correlates well with definitions based on gold-standard Cy5.5 analysis, increasing confidence that the quantification data presented elsewhere in the manuscript is accurate.*

The next question relates to what type of cell a porcine $CD163^+CD14^-$ monocyte represents, and what the equivalent cell type would be in mice. As the Reviewer suggests, there are substantial differences in the expression of surface markers between porcine and murine monocytes, with significantly fewer studies conducted in pigs that extrapolate to the human system. Pig monocyte populations tend to be described based on reciprocal expression of CD14 and the scavenger receptor CD163, while mouse monocytes tend to be categorized based on Ly6C/CX3CR1 status and human monocytes based on CD14 and CD16[8]. $CD163^-CD14^+$ and $CD163^+CD14^-$ are considered components of a maturation series controlled by the growth factor, CSF1. While $CD163^-CD14^+$ monocytes are typically considered to display a classical inflammatory monocyte phenotype, the $CD163^+CD14^-$ subpopulation appears to have an intermediate phenotype that shares properties with both the classical and non-classical human monocyte populations[8]. It is unclear whether porcine $CD163^+CD14^-$ monocytes reflect the Ly6C intermediate population found in mice[9], or if they are more similar to the Ly6C high population of inflammatory monocytes known to infiltrate the atherosclerotic plaque[4,10].

What is known is that porcine CD163$^+$CD14$^-$ cells comprise a more mature set of monocytes, with phenotypic characteristics that parallel CD14$^+$CD16$^+$ intermediate human monocytes[11]. Similar to CD14$^+$CD16$^+$ monocytes that are functionally defined by roles in transendothelial migration, phagocytosis, and antigen presentation[12], pig CD163$^+$CD14$^-$ monocytes express significantly higher levels of cell adhesion molecules including CD11a and CD11R1, highlighting their potential role in adhesion to the diseased vessel wall and rapid extravasation from the circulation into the developing plaque[11]. The phenotype of these CD163$^+$CD14$^-$ monocytes potentially explains their relatively low percentage in blood relative to other circulating populations[8]. At the same time, CD163$^+$CD14$^-$ monocytes have been reported to actively participate in antigen presentation to T cells and to elaborate high levels of the inflammatory cytokine, TNFa[12,13]. CD163 mRNA and protein expression were found to be elevated in colonic biopsies from patients with ulcerative colitis and Crohn's disease compared to healthy controls[14]. Similarly, in pigs infected with Actinobacillus pleuropneumoniae to induce pneumonia, there was significant infiltration of CD163$^+$ monocytes into the tracheobronchial lymph nodes of infected pigs[15]. Thus, this inflammatory subset of porcine monocytes functionally comports with the inflammatory subset of murine monocytes known to avidly take up SWNTs and rapidly traffic them to the developing atherosclerotic plaque as well as human intermediate monocytes involved in transendothelial migration, cardiovascular disease, and antigen presentation[4,11]. Given that as few as 85 dendritic cells have been estimated to be sufficient to activate a robust immune response[16], it is possible that this relatively low prevalence monocytic cell population is capable of trafficking to the vasculature and producing the anti-inflammatory response observed in vivo.

*To specifically test the hypothesis that nanoparticle-laden monocytes may exit the circulation and deliver meaningful concentrations of SWNT to the inflamed blood vessel, we next performed flow cytometric analyses of dissociated vascular samples and compared rates of SWNT accumulation in monocytes and macrophages relative to other cell types. As shown in **Figure S**, we observed significant enrichment and accumulation in MO/MΦ isolated from multiple vascular beds, including the carotid artery, iliac artery, and the renal artery bifurcation.*

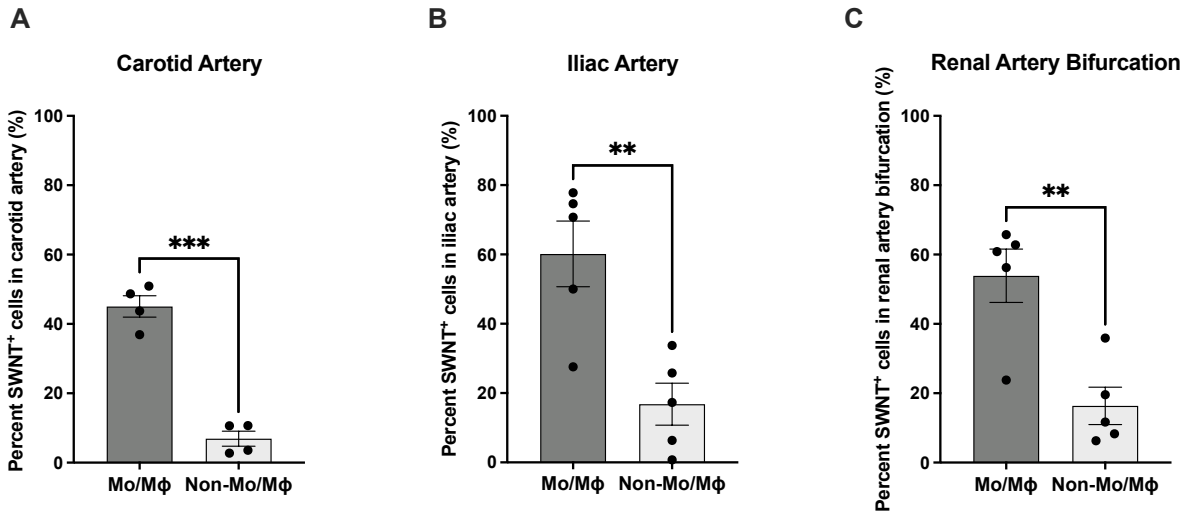

Figure S. SWNTs/SWNT-SHP1i were selectively taken up by the MO/MΦ population of vascular tissues containing early atherosclerotic lesions. A) SWNT$^+$ cells in the carotid artery (n=4, ***p=0.0001); B) SWNT$^+$ cells in the Iliac artery (n=5, **p<0.01); C) SWNT$^+$ cells in the renal artery bifurcation (n=5, **p<0.01). Statistical analyses were performed using an unpaired T test with Welch's Correction.

*In contrast, few SWNTs were observed in the bone marrow of pigs treated with SWNT or SWNT-SHP1i (including samples from the new Cy5.5-treated animals shown in red), regardless of cell type analyzed (**Figure T**).*

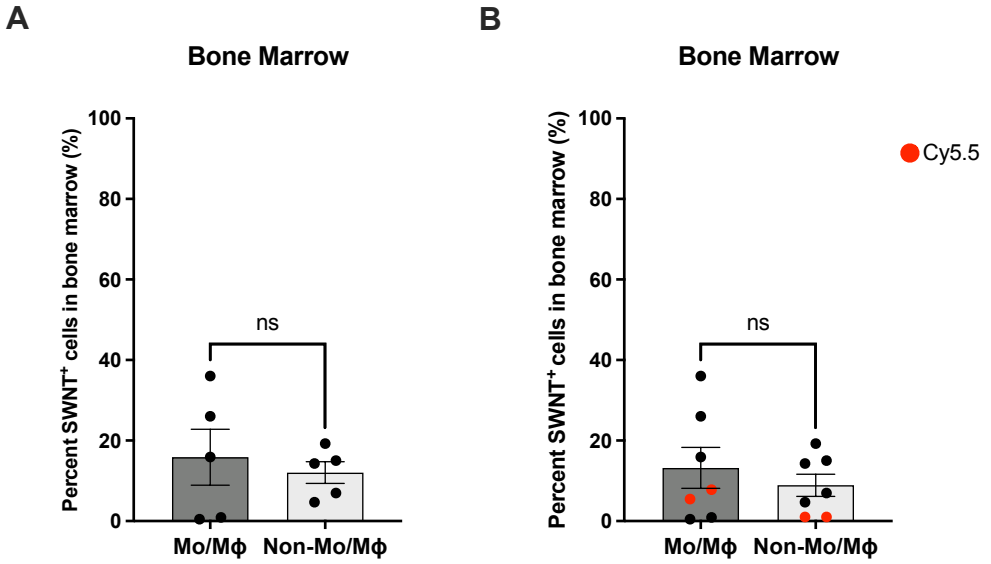

Figure T. SWNTs/SWNT-SHP1i were not extensively taken up by the MO/MΦ population of the bone marrow. A) SWNT$^+$ cells in the bone marrow (n=5, p=0.6314). B) SWNT$^+$ cells in the bone marrow, including from Cy5.5 treated pigs indicated in red (n=7, p=0.4753). Statistical analysis was performed using an unpaired T test with Welch's Correction.

Together, these data suggest that, while a rare subpopulation of cells in the circulation, those monocytes which do take up SWNTs are effective at delivering them to the end organ, and that they accumulate to a meaningful extent within the phagocytic cells that comprise the developing atherosclerotic lesion. We thank the Reviewer for the opportunity to clarify this concept and confirm significant delivery of our pro-efferocytic therapy to the inflamed blood vessel.

2. Figure 2. If pieces of straight segments of the carotid artery are used, they are not likely to contain any atherosclerosis at this early stage of plaque development, because the straight segments of common carotid arteries are not atherosclerosis-prone regions. In that case, the cells should not be referred to as intraplaque cells.

***Response:** We appreciate Reviewer #4's question regarding the regions of the carotid artery used in our manuscript. We believe this is in reference to Figures 3 and 4, as Figure 2 describes flow cytometry data of pig blood. In the revised text, we now clarify that our RNA-sequencing studies were performed on tissue harvested from the common carotid artery, rather than from the bifurcation of the carotid artery. We also note that all histology studies were performed on coronary artery specimens, specifically at the ostium where plaques were most consistently observed. For the original FDG-PET/CT analysis, the ROI was indeed drawn along and included the straight segment of the common carotid artery (CCA).*

*However, we fully agree with the Reviewer that an assessment of vascular inflammation including the carotid bifurcation might provide more accurate insights specific to biology occurring in the most atherosclerosis-prone regions of the vessel (**Figure U**). Accordingly, we have now performed a blinded*

analysis of each carotid bifurcation, capturing the SUV_{mean} signal extending from the straight segment of the common carotid artery through the proximal portions of the internal and external carotid arteries.

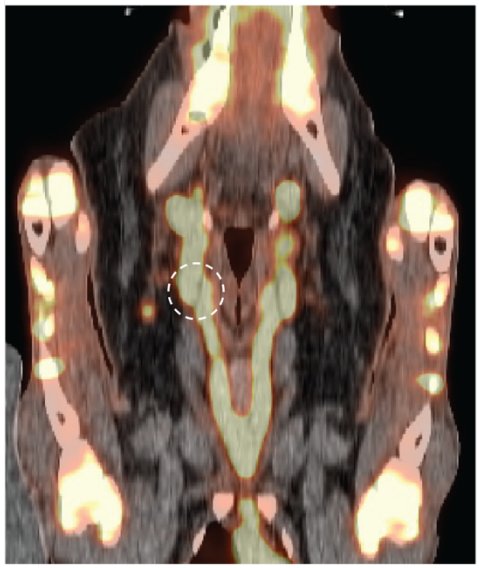

Figure U. PET/CT (coronal image) delineating the PET signal at the carotid bifurcation. Analysis extends from the proximal CCA into the proximal ICA and ECA.

These analyses revealed a significant difference in both the pooled and averaged RCA + LCA SUV_{mean} between SWNT-SHP1i and SWNT groups (see Figure V below). Consistent with the Reviewer's comment, we believe these observed differences reflect the early plaques developing in this atheroprone region, and the potent anti-inflammatory effects of SWNT-SHP1i delivered to this site.

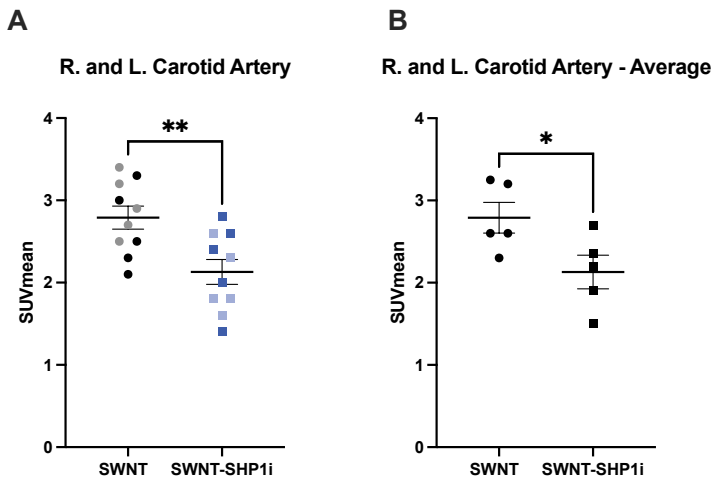

Figure V. Analysis of vascular inflammation at the carotid bifurcation in SWNT and SWNT-SHP1i treated animals. A) SUV_{mean} of the pooled RCA and LCA (n=10/group, **p<0.01); B) SUV_{mean} of the averaged RCA and LCA (n=5/group, *p<0.05).

3. Figure 3. There are only very early changes in the intima and the authors should avoid calling this atherosclerotic plaque. However, it would be highly interesting to test this therapy in animals with proper

atherosclerotic plaques, and this should be possible as an intervention trial after plaques are induced by long-term high-fat diet feeding.

Response: *We fully agree with Reviewer 4's comment and have revised the manuscript to highlight that most of our observations were made in atheroprone vessels harboring fatty streaks and early atherosclerotic lesions rather than advanced atherosclerotic plaques. We also agree that an additional study of longer duration in older animals with established lesions would be hugely informative and extend the findings of the current manuscript. To explore this possibility, we reached out to the company that provided us our research animals and formulated a budget for such a study. We determined that extending our study from 3 months to 6 months would cost an additional $211,866 in pig procurement/housing/Western diet fees and an additional $262,669 in SWNT manufacturing costs. These costs are exclusive of PET/CT imaging fees, RNA-sequencing, veterinary/anesthesia fees, Cy5.5 imaging probe ($9,520/dose/pig), and any support for laboratory personnel/post-docs. While we of course would like very much to pursue this additional study, our academic laboratories unfortunately do not have access to the funds (which would likely exceed $1M) needed to conduct this work. Having said that, we are now in communication with a private company that has expressed interest in developing our nanoparticles for clinical study and are actively working with them to design an additional, longer-term study, and hope that this work will begin in the coming months. We now more clearly emphasize this as an area for future directions, which will enable the translation of this discovery into prospective clinical trials.*

4. Figure 3e. A critical requirement for the t-test is that observations are independent, but they are not in this case, where each animal contributes two data points. This inflates the type 1 error. Instead, the average should be used which would mean n=5 in each group, and therefore likely no statistical difference. Please also report signal intensities from a neighboring vein or the heart ventricles to demonstrate that carotid SUV differences are not coming from background differences.

Response: *We appreciate the Reviewer's feedback regarding the statistical approach applied to analyze the PET/CT results. In our reanalysis including the carotid bifurcation, we average the RCA and LCA as recommended by the Reviewer and find a significant decrease in the SWNT-SHP1i vascular inflammation compared to SWNT controls (p = 0.0438) using an unpaired T test with Welch's correction.*

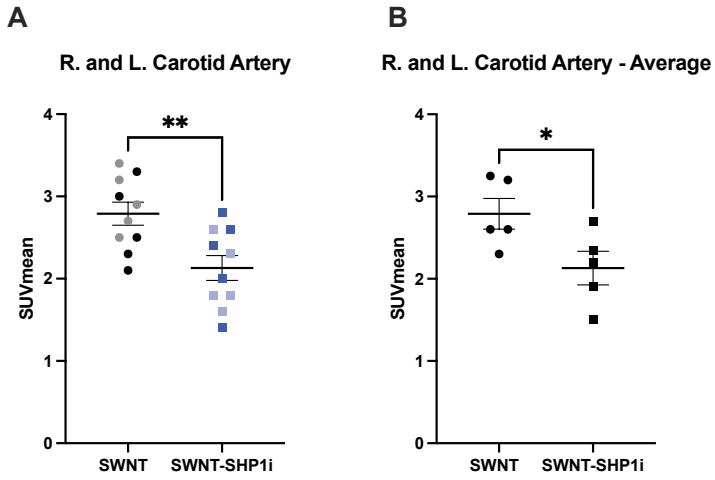

Figure V. Analysis of vascular inflammation at the carotid bifurcation in SWNT and SWNT-SHP1i treated animals. A) SUV_{mean} of the pooled RCA and LCA (n=10/group, **p<0.01); B) SUV_{mean} of the averaged RCA and LCA (n=5/group, *p<0.05).

*Notably, the background signal intensities from both the left ventricle and right forelimb muscle are equivalent in the SWNT and SWNT-SHP1i cohorts (**Figure W**), arguing that the improvements observed in the vasculature were not due to artifact or background differences.*

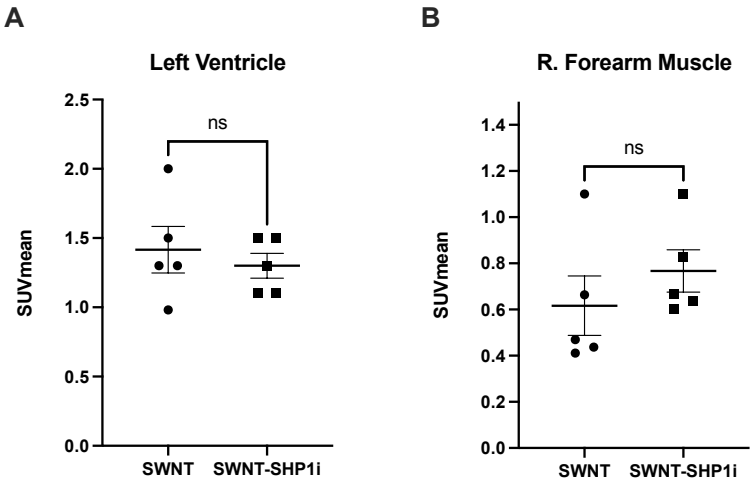

Figure W. No significant differences were observed in the background signal intensities of the A) Left ventricle (n=5, p=0.5635) or B) Right forearm muscle (n=5, p=0.3720) between SWNT and SWNT-SHP1i treated pigs.

Also of note, these results are consistent with ^{18}F-FDG PET/CT data included in our previously published Nature Nanotechnology study[4]. In that report, mice treated with SWNT-SHP1i demonstrated a significant reduction in vascular inflammation of the aorta compared to SWNT controls, similar to what we observed in the current large animal experiments.

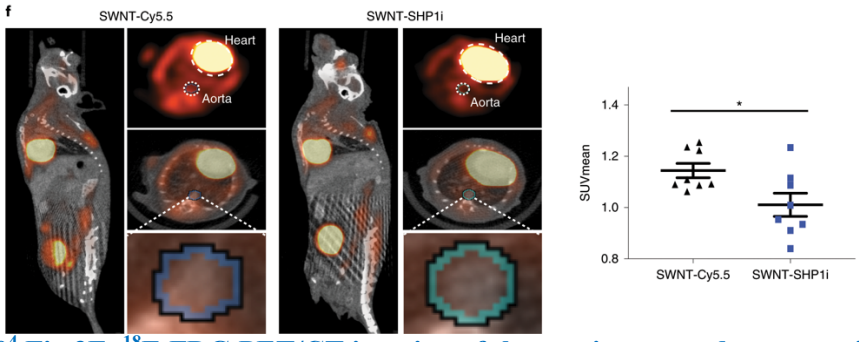

Flores et al. 2020[4] Fig 3F: ^{18}F-FDG PET/CT imaging of the murine aorta demonstrating a significant reduction in vascular inflammation in SWNT-SHP1i treated mice compared to SWNT treated controls (*p<0.05).

5. Figure 3f. There is no significant change in intimal macrophages. Concluding that there is a trend at p=0.46 seems unjustified.

***Response**: We acknowledge the Reviewer's point and have modified the conclusion to reflect that there was no significant change in intimal macrophages. We now write "Although there was no significant difference in macrophage recruitment in SWNT-SHP1i-treated atherosclerotic lesions (Fig. 3e, p = 0.4339), lesions from SWNT-SHP1i treated animals harbored significantly fewer TUNEL-positive apoptotic bodies (Fig. 3f, *p <0.05), suggesting enhanced clearance of cells, which would otherwise accumulate within the developing necrotic core."*

5. Figure 3g. It is surprising that the small dots can amount to 3 percent of the lesion area, and it would in any case be a better measure to count Tunel/Dapi+ signal and provide the ratio against total Dapi+ cells. Also, please note that for the statistical test used, the assumption of equal variance in the t-test is not fulfilled.

Response: *We fully agree and appreciate the opportunity to address the Reviewer's comment. In response, we have now calculated the percentage of TUNEL+ cells per DAPI+ nucleus. Similar to the original TUNEL analyses, we found a significant difference between the SWNT and SWNT-SHP1i groups (*p <0.05), which were normally distributed (**Figure X**). Statistical analysis was performed using Welch's T test.*

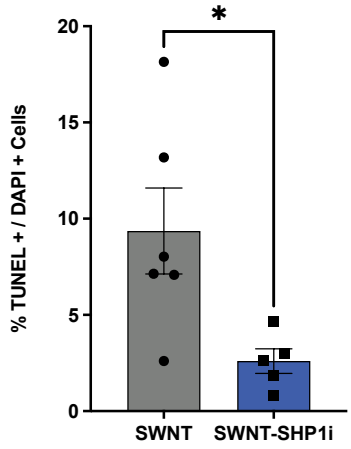

Figure X. The % of TUNEL$^+$ cells per DAPI$^+$ nucleus within the right coronary artery ostium was calculated for SWNT (n=6) and SWNT-SHP1i (n=5) treated pigs (*p<0.05).

6. If slower infusion of the therapy has been part of the solution for avoiding the pigs dying on the operating table, the authors should consider whether they are caused by the CARPA reaction, which is often observed in pigs after the infusion of nanoparticles.

Response*: We appreciate the Reviewer's suggestion to consider the potential role of complement activation-related pseudo allergy (CARPA). CARPA has been proposed to occur by a double-hit hypothesis involving both complement and macrophage activation[16,17]. To evaluate for the presence of downstream CARPA sequelae, we first sought to evaluate for the presence of microvascular thrombosis or macrophage infiltration within the lung. We analyzed pulmonary morphometry by H&E and stained for macrophages using IBA-1 and found no increase in the % of IBA-1 positive area normalized to the total lung area in the pigs that died during the experimental protocol (**Figure Y**). The absence of macrophage activation in the lung tissue of deceased pigs reduces our suspicion that CARPA contributed to these deaths.*

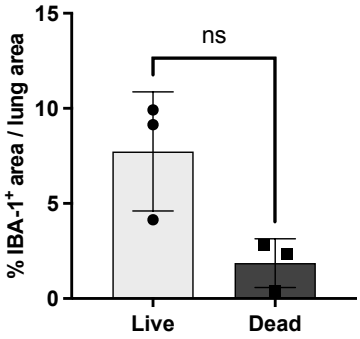

Figure Y. The % of IBA-1$^+$ cells per lung area calculated for pigs receiving the full 12 weeks of treatment (n=3) and pigs that died before sacrifice (n=3; p = 0.0674).

*Furthermore, review of available anesthesia records indicated that the animals that died did not demonstrate signs of hypotension as might be expected in anaphylaxis or hemodynamic collapse in the setting of CARPA (**Figure Z**). After adjustment of the anesthesia protocol by the veterinary team (who had been administering bolus sedative injections to expedite drug infusions and blood draws and noted respiratory depression), we observed no further deaths in either cohort. Together, these data reduced our suspicion that CARPA was the cause of death for the three pigs in our study (SWNT n=2; SWNT-SHP1i n=1).*

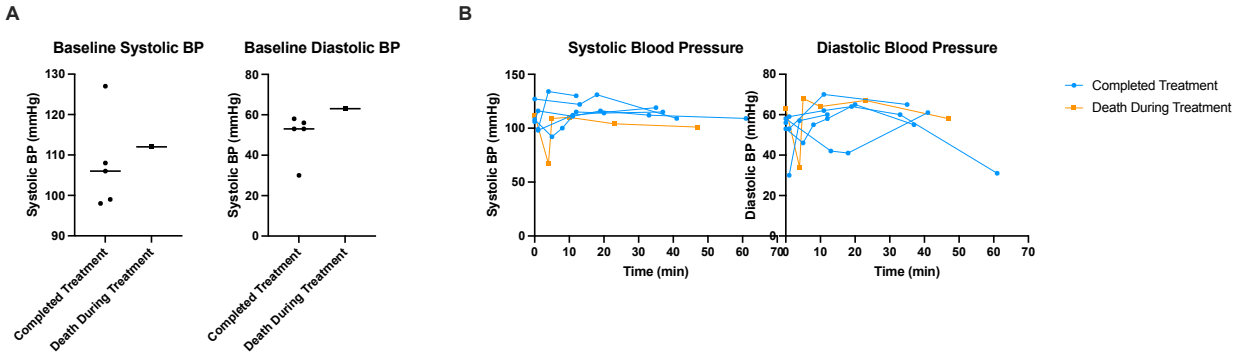

Figure Z. Systolic and diastolic blood pressure measurement in pigs undergoing SWNT and SWNT-SHP1i transfusion (Week 5). A) Baseline systolic and diastolic BP (mmHg) of alive (n=5) versus prematurely deceased pigs (n=1); B) Systolic and diastolic BP measurements during SWNT/SWNT-SHP1i infusion at Week 5 of treatment in alive (n=5) versus prematurely deceased pigs (n=1).

Minor issues

1. Figure 1. The small graphs at the top showing which subpopulation is being examined appear to be switched in some cases. Furthermore, it would be helpful with some kind of explanation of how the SWNT gate is set and why it looks different in the different analyses.

***Response:** We thank the Reviewer for noticing this issue and apologize for this inadvertent error (which we presume is in reference to Figure 2). We have now reviewed and adjusted the labeling of the Figure 2 graphs. Moreover, we incorporated several other changes in these graphs as suggested by other Reviewers (including providing clearer gating examples, compensation controls, and unstained controls). The reason why the SWNT gate appeared different in certain cell types was that the baseline background fluorescence levels of each cell type may differ. We determined the gate location in each cell type individually using baseline blood samples from untreated pigs (never exposed to SWNT or SWNT-SHP1i) as controls. Any*

signal in the SWNT channel observed in untreated blood was considered as the biological baseline and gates were set beyond that background signal in each cell type. The Methods have now been updated to more carefully explain how these analyses were conducted.

2. Figure 2. Please explain how the gate for $SWNT^+$ cells was set.

Response: *As outlined above, the $SWNT^+$ gate for each cell type was set using baseline blood from untreated pigs. These baseline samples from animals which were never exposed to SWNTs were processed, stained, and recorded on the flow cytometer using our staining panels, with appropriate compensation controls. Any signal suggesting staining with the anti-PEG antibody (which defines the presence of SWNTs) in these untreated samples was considered to be background staining, and defined as zero, with gates set accordingly. Thereafter, positive signal in the treated animals was deemed to reflect a SWNT-positive cell.*

3. In the methods description for the pigs, it is written as if the gene modification was created anew in this batch of pigs, but they were probably bred from gene-modified founders. Please clarify.

Response: *We appreciate the Reviewer's suggestion and have clarified this point in the Methods ('Experimental Animals' section). Indeed, the LDLR $^{-/-}$ and control LDLR $^{+/+}$ mini-Yucatan pigs obtained from Exemplar Genetics, IA, USA have been described in prior publications and were not a newly generated strain of animals developed solely for this report[18]. The animals utilized in this study were generated for us via somatic cell nuclear transfer (cloning) using LDLR-/- cells.*

4. Figure 3d. Mice are mentioned.

Response: *We thank the Reviewer for pointing out this typo. Figure 3d has been revised to reflect that the experiments were conducted in pigs.*

References

1. Davis K., Kristen N., Sood A. Amgen Presents Results Highlighting The Long-Term Safety And Efficacy Of Repatha® (Evolocumab) In The Longest Duration Study Of A PCSK9 Inhibitor To Date At AHA Scientific Sessions 2018. Amgen (2018).
2. Fala L. Repatha (Evolocumab): Second PCSK9 Inhibitor Approved by the FDA for Patients with Familial Hypercholesterolemia. *Am Health Drug Benefits* **9,** 136-139 (2016).
3. Vaidyanathan S., Patel C. N., Scarsbrook A. F., Chowdhury F. U. FDG PET/CT in infection and inflammation--current and emerging clinical applications. *Clin Radiol* **70,** 787-800 (2015).
4. Flores A. M., et al. Pro-efferocytic nanoparticles are specifically taken up by lesional macrophages and prevent atherosclerosis. *Nat Nanotechnol* **15,** 154-161 (2020).
5. Rokkam V. R., Killeen R. B., Kotagiri R. Secondary Thrombocytosis. StatPearls. Treasure Island (FL): StatPearls Publishing Copyright © 2024, StatPearls Publishing LLC (2024).
6. Kunutsor S. K., Apekey T. A., Khan H. Liver enzymes and risk of cardiovascular disease in the general population: a meta-analysis of prospective cohort studies. *Atherosclerosis* **236,** 7-17 (2014).
7. Smith B. R., et al. Selective uptake of single-walled carbon nanotubes by circulating monocytes for enhanced tumour delivery. *Nature nanotechnology* **9,** 481-487 (2014).
8. Fairbairn L., et al. Comparative analysis of monocyte subsets in the pig. *J Immunol* **190,** 6389-6396 (2013).
9. Sunderkötter C., et al. Subpopulations of mouse blood monocytes differ in maturation stage and inflammatory response. *J Immunol* **172,** 4410-4417 (2004).
10. Robbins C. S., et al. Extramedullary hematopoiesis generates Ly-6C(high) monocytes that infiltrate atherosclerotic lesions. *Circulation* **125,** 364-74 (2012).
11. Kapellos TS, Bonaguro L, Gemünd I, et al. Human Monocyte Subsets and Phenotypes in Major Chronic Inflammatory Diseases. *Front Immunol* **10,** 2035 (2019).
12. Chamorro S., Revilla C., Alvarez B., Alonso F., Ezquerra A., Domínguez J.. Phenotypic and functional heterogeneity of porcine blood monocytes and its relation with maturation. *Immunology* **114,** 63-71 (2005).
13. Chamorro S., Revilla C., Alvarez B., López-Fuertes L., Ezquerra A., Domínguez J. Phenotypic characterization of monocyte subpopulations in the pig. *Immunobiology* **202,** 82-93 (2000).
14. Franzè E., et al. Lesional accumulation of CD163-expressing cells in the gut of patients with inflammatory bowel disease. *PLoS One* **8,** e69839 (2013).
15. Ondrackova P., Leva L., Kucerova Z., Vicenova M., Mensikova M., Faldyna M. Distribution of porcine monocytes in different lymphoid tissues and the lungs during experimental Actinobacillus pleuropneumoniae infection and the role of chemokines. *Vet Res* **44,** 98 (2013).
16. Csukás D., Urbanics R., Wéber G., Rosivall L., Szebeni J. Pulmonary intravascular macrophages: prime suspects as cellular mediators of porcine CARPA. *European Journal of Nanomedicine* **7,** 27-36 (2015).
17. Szebeni J., Simberg D., González-Fernández Á., Barenholz Y., Dobrovolskaia M. A. Roadmap and strategy for overcoming infusion reactions to nanomedicines. Nat Nanotechnol **13,** 1100-1108 (2018).

18. Davis B. T., et al. Targeted disruption of LDLR causes hypercholesterolemia and atherosclerosis in Yucatan miniature pigs. *PLoS One* **9,** e93457 (2014).

Supplemental Table 1. Pig Bulk RNA-Sequencing DEGs

Gene ID	log2FoldChange	P Value	Adjusted P value	Gene Abbreviation
ENSSSCG00000002782	5.63	1.49E-05	0.01	PLEKHG4
ENSSSCG00000039745	4.98	3.16E-06	2.09E-03	HMOX1
ENSSSCG00000039798	4.49	6.56E-06	3.70E-03	SLC11A1
ENSSSCG00000056276	4.28	4.85E-04	0.04	SLAMF9
ENSSSCG00000038688	3.90	1.49E-07	4.54E-04	PGLYRP1
ENSSSCG00000028331	3.90	3.42E-04	0.04	IL1R2
ENSSSCG00000025993	3.62	3.61E-04	0.04	SGPP2
ENSSSCG00000002032	3.50	5.73E-07	9.69E-04	SLC7A8
ENSSSCG00000044075	3.40	5.45E-04	0.05	No ID
ENSSSCG00000032438	3.35	2.24E-08	8.66E-05	FFAR2
ENSSSCG00000006588	3.34	4.21E-04	0.04	S100A9
ENSSSCG00000029960	3.28	6.06E-04	0.05	LRRC4B
ENSSSCG00000029414	3.21	2.21E-05	0.01	FCN1
ENSSSCG00000038351	2.99	4.60E-04	0.04	TNFRSF18
ENSSSCG00000062991	2.98	1.37E-04	0.02	KCNK12
ENSSSCG00000036132	2.93	1.81E-08	8.66E-05	CKM
ENSSSCG00000014259	2.87	2.11E-05	0.01	ADAMTS19
ENSSSCG00000003846	2.81	3.15E-04	0.04	GLIS1
ENSSSCG00000015246	2.81	2.00E-05	0.01	ST14
ENSSSCG00000009929	2.78	3.40E-06	2.15E-03	TRPV4
ENSSSCG00000021569	2.77	1.40E-04	0.02	MMP25
ENSSSCG00000032241	2.76	1.72E-06	1.31E-03	GPNMB
ENSSSCG00000022236	2.70	1.06E-06	1.09E-03	FOLR3
ENSSSCG00000031155	2.70	5.68E-07	9.69E-04	RASD2
ENSSSCG00000000106	2.67	1.24E-05	0.01	KCNJ4
ENSSSCG00000025795	2.65	1.61E-05	0.01	CSF3R
ENSSSCG00000008318	2.61	3.71E-04	0.04	VAX2
ENSSSCG00000014310	2.58	1.36E-04	0.02	CXCL14
ENSSSCG00000036352	2.54	2.11E-05	0.01	RAB7B
ENSSSCG00000039322	2.52	1.11E-06	1.09E-03	NRGN
ENSSSCG00000026890	2.52	5.85E-04	0.05	GALNT6
ENSSSCG00000040080	2.50	8.12E-09	8.66E-05	PTGDS
ENSSSCG00000030088	2.48	9.70E-07	1.09E-03	CSF2RA
ENSSSCG00000013556	2.43	5.35E-04	0.05	ADGRE1
ENSSSCG00000022739	2.43	2.52E-04	0.03	DSG2
ENSSSCG00000059775	2.40	1.55E-06	1.29E-03	LOC100624191
ENSSSCG00000006287	2.39	4.72E-06	2.76E-03	SELL

ENSSSCG00000053501	2.35	3.36E-04	0.04	FOLR1
ENSSSCG00000008240	2.32	3.85E-04	0.04	SH2D6
ENSSSCG00000008937	2.30	9.69E-05	0.02	AMBN
ENSSSCG00000040981	2.29	9.54E-05	0.02	GMFG
ENSSSCG00000017540	2.27	6.53E-05	0.01	HOXB5
ENSSSCG00000051406	2.23	2.17E-05	0.01	No ID
ENSSSCG00000013237	2.22	3.33E-04	0.04	SPI1
ENSSSCG00000024310	2.21	2.54E-06	1.76E-03	F13A1
ENSSSCG00000017956	2.18	2.75E-05	0.01	CD68
ENSSSCG00000009314	2.16	5.33E-04	0.05	FLT3
ENSSSCG00000011322	2.16	1.42E-04	0.02	CCR1
ENSSSCG00000015612	2.15	3.51E-05	0.01	IRF6
ENSSSCG00000010948	2.14	3.52E-04	0.04	CTSL
ENSSSCG00000017258	2.08	3.93E-04	0.04	FAM20A
ENSSSCG00000033146	2.07	1.15E-06	1.09E-03	CD163
ENSSSCG00000006472	2.07	5.37E-05	0.01	CRABP2
ENSSSCG00000013579	2.05	5.06E-04	0.04	CD209
ENSSSCG00000014369	2.03	2.98E-05	0.01	CD14
ENSSSCG00000032355	2.03	3.22E-04	0.04	LY86
ENSSSCG00000027928	2.02	3.29E-04	0.04	TMEM9
ENSSSCG00000001849	1.98	5.22E-05	0.01	ANPEP
ENSSSCG00000003584	1.93	3.94E-04	0.04	THEMIS2
ENSSSCG00000002452	1.93	5.77E-05	0.01	LGMN
ENSSSCG00000021748	1.93	6.20E-04	0.05	PRR5
ENSSSCG00000044583	1.93	4.07E-05	0.01	LRG6
ENSSSCG00000013041	1.92	4.73E-04	0.04	FERMT3
ENSSSCG00000014136	1.91	8.89E-07	1.09E-03	VCAN
ENSSSCG00000012278	1.88	2.54E-04	0.03	CFP
ENSSSCG00000031487	1.87	3.61E-04	0.04	LSP1
ENSSSCG00000033444	1.87	3.01E-04	0.04	SPC24
ENSSSCG00000025644	1.85	5.12E-04	0.04	pCD1A
ENSSSCG00000006979	1.85	4.07E-04	0.04	MSR1
ENSSSCG00000014843	1.85	3.13E-04	0.04	CHRDL2
ENSSSCG00000000137	1.84	6.10E-05	0.01	NCF4
ENSSSCG00000003278	1.82	2.23E-05	0.01	No ID
ENSSSCG00000001582	1.81	7.14E-06	3.88E-03	MDGA1
ENSSSCG00000016784	1.81	6.23E-05	0.01	ANKH
ENSSSCG00000017585	1.79	2.13E-04	0.03	SAMD14
ENSSSCG00000029715	1.79	1.34E-06	1.20E-03	OLFM

ENSSSCG00000013901	1.78	2.31E-04	0.03	IFI30
ENSSSCG00000025133	1.77	2.94E-04	0.04	ITGB2
ENSSSCG00000021557	1.77	1.33E-04	0.02	R-SSC-9748784
ENSSSCG00000007586	1.76	4.89E-04	0.04	FSCN1
ENSSSCG00000006357	1.75	6.42E-05	0.01	FCER1G
ENSSSCG00000015037	1.75	1.29E-04	0.02	IL18
ENSSSCG00000007240	1.74	4.14E-05	0.01	HCK
ENSSSCG00000032181	1.74	2.36E-04	0.03	C17orf58
ENSSSCG00000016343	1.72	2.27E-04	0.03	TWIST2
ENSSSCG00000023630	1.72	2.20E-04	0.03	CPM
ENSSSCG00000021238	1.68	3.43E-07	8.69E-04	STX1B
ENSSSCG00000005762	1.68	4.10E-04	0.04	KCNT1
ENSSSCG00000009589	1.68	2.55E-04	0.03	SYK
ENSSSCG00000037351	1.67	4.95E-04	0.04	LOC110257072
ENSSSCG00000008723	1.67	2.28E-08	8.66E-05	HTRA3
ENSSSCG00000013049	1.65	1.66E-05	0.01	RCOR2
ENSSSCG00000025537	1.64	3.69E-04	0.04	PTPN6
ENSSSCG00000011436	1.63	5.62E-04	0.05	TLR9
ENSSSCG00000015735	1.63	2.30E-04	0.03	PTPN18
ENSSSCG00000001427	1.63	1.40E-04	0.02	R-SSC-8957275
ENSSSCG00000027826	1.62	1.96E-05	0.01	GIMAP4
ENSSSCG00000060622	1.60	8.02E-07	1.09E-03	IFITM1
ENSSSCG00000022794	1.59	2.80E-04	0.04	HHIPL1
ENSSSCG00000056729	1.58	1.64E-05	0.01	C5AR1
ENSSSCG00000022004	1.58	3.96E-04	0.04	SH3BP2
ENSSSCG00000055678	1.58	3.67E-04	0.04	C1QTNF6
ENSSSCG00000011364	1.58	2.05E-04	0.03	NCKIPSD
ENSSSCG00000012893	1.57	5.53E-05	0.01	UNC93B1
ENSSSCG00000005284	1.57	1.06E-04	0.02	GNA14
ENSSSCG00000038801	1.56	3.10E-04	0.04	NPNT
ENSSSCG00000017754	1.55	8.86E-06	4.21E-03	LGALS9
ENSSSCG00000039245	1.55	3.62E-05	0.01	RIMS3
ENSSSCG00000005641	1.54	1.12E-04	0.02	DNM1
ENSSSCG00000007739	1.54	1.63E-04	0.03	GUSB
ENSSSCG00000001782	1.53	1.68E-04	0.03	ABHD17C
ENSSSCG00000037466	1.53	4.57E-04	0.04	No ID
ENSSSCG00000003931	1.51	5.25E-04	0.05	KIF2C
ENSSSCG00000035195	1.51	7.10E-05	0.01	HNMT
ENSSSCG00000033913	1.50	2.59E-04	0.03	C1RL

ENSSSCG00000005638	1.49	3.78E-04	0.04	LCN2
ENSSSCG00000016859	1.48	5.83E-04	0.05	C7
ENSSSCG00000040162	1.46	2.40E-04	0.03	NUPR1
ENSSSCG00000036747	1.46	4.69E-04	0.04	WAS
ENSSSCG00000017355	1.44	3.70E-04	0.04	GRN
ENSSSCG00000015405	1.43	1.31E-04	0.02	LOC100511343
ENSSSCG00000000292	1.42	3.00E-04	0.04	ZNF385A
ENSSSCG00000029949	1.42	8.44E-06	4.14E-03	CD248
ENSSSCG00000016823	1.41	1.61E-06	1.29E-03	C1QTNF3
ENSSSCG00000001727	1.41	1.89E-05	0.01	TNFRSF21
ENSSSCG00000016573	1.40	4.54E-04	0.04	IRF5
ENSSSCG00000005680	1.40	4.23E-04	0.04	PRRX2
ENSSSCG00000009880	1.40	3.74E-04	0.04	SLC8B1
ENSSSCG00000035299	1.39	1.47E-04	0.02	SFRP4
ENSSSCG00000026383	1.39	2.83E-04	0.04	NRP2
ENSSSCG00000034284	1.38	3.63E-04	0.04	LOC100515837
ENSSSCG00000053991	1.37	4.09E-04	0.04	SOX12
ENSSSCG00000035170	1.36	2.98E-04	0.04	VSIG4
ENSSSCG00000000907	1.36	2.50E-05	0.01	PLXNC1
ENSSSCG00000009664	1.36	5.38E-05	0.01	PTK2B
ENSSSCG00000025826	1.32	4.65E-04	0.04	BOC
ENSSSCG00000052303	1.32	5.82E-04	0.05	RAB32
ENSSSCG00000011443	1.29	4.16E-04	0.04	STAB1
ENSSSCG00000061268	1.29	4.32E-07	9.39E-04	IFIT3
ENSSSCG00000007565	1.29	4.71E-05	0.01	TTYH3
ENSSSCG00000029230	1.28	2.37E-04	0.03	ECM1
ENSSSCG00000000368	1.25	2.41E-04	0.03	MMP19
ENSSSCG00000012853	1.24	2.09E-05	0.01	IRF7
ENSSSCG00000014441	1.23	3.54E-04	0.04	CSF1R
ENSSSCG00000025686	1.20	1.50E-04	0.02	KMO
ENSSSCG00000033512	1.19	4.05E-04	0.04	C1QB
ENSSSCG00000007146	1.18	2.66E-04	0.04	SIGLEC1
ENSSSCG00000016298	1.18	3.76E-04	0.04	INPP5D
ENSSSCG00000003366	1.18	1.36E-04	0.02	CHD5
ENSSSCG00000013074	1.17	4.90E-04	0.04	RAB3IL1
ENSSSCG00000046640	1.14	8.39E-07	1.09E-03	OAS1
ENSSSCG00000036135	1.12	3.80E-04	0.04	COL1A1
ENSSSCG00000026863	-1.07	2.79E-04	0.04	FARP1
ENSSSCG00000041935	-1.13	6.27E-04	0.05	HSPB7

ENSSSCG00000062876	-1.17	3.58E-04	0.04	SLC25A30
ENSSSCG00000007139	-1.24	5.80E-04	0.05	ADRA1D
ENSSSCG00000016200	-1.28	2.92E-04	0.04	PRKAG3
ENSSSCG00000040636	-1.32	2.90E-04	0.04	KRT80
ENSSSCG00000014927	-1.43	1.56E-04	0.03	NOX4
ENSSSCG00000011973	-1.50	8.62E-05	0.02	COL8A1
ENSSSCG00000011524	-1.55	7.06E-05	0.01	CHL1
ENSSSCG00000030998	-1.58	7.67E-06	4.02E-03	WIF1
ENSSSCG00000000810	-1.72	2.51E-04	0.03	AMIGO2
ENSSSCG00000026600	-1.76	8.37E-06	4.14E-03	KLHL30
ENSSSCG00000005494	-1.85	2.47E-04	0.03	TNC
ENSSSCG00000003640	-1.87	2.33E-05	0.01	GRIK3
ENSSSCG00000024954	-1.91	6.25E-05	0.01	FGF1
ENSSSCG00000012026	-2.00	3.16E-04	0.04	ADAMTS1
ENSSSCG00000013088	-2.02	2.29E-04	0.03	LRRC10B
ENSSSCG00000003414	-2.05	4.54E-06	2.76E-03	ANGPTL7
ENSSSCG00000004340	-2.06	4.80E-05	0.01	FHL5
ENSSSCG00000010256	-2.15	7.01E-05	0.01	COL13A1
ENSSSCG00000001832	-2.24	2.26E-06	1.64E-03	ACAN
ENSSSCG00000015334	-2.28	3.26E-05	0.01	PDK4
ENSSSCG00000017508	-2.40	1.44E-04	0.02	STAC2
ENSSSCG00000010144	-2.48	1.82E-05	0.01	ACTN2
ENSSSCG00000027301	-2.64	4.78E-04	0.04	No ID
ENSSSCG00000037190	-2.80	5.71E-04	0.05	TAGLN3
ENSSSCG00000011640	-6.50	5.13E-05	0.01	TF

REVIEWERS' COMMENTS

Reviewer #1 (Remarks to the Author):

The authors have greatly improved the revised manuscript to address most of the concerns from the previous round of review. While there were some remaining concerns such as questions regarding the large animal model, to fully address these would require a significant delay and extensive resources that would unduly interfere with the timely publication of these potentially important findings.

Reviewer #2 (Remarks to the Author):

The authors have adressed all the comments, and I recommend this manuscript to be published in Nature Communications.

Reviewer #3 (Remarks to the Author):

The authors have adequately addressed my concerns.

The PET images in Fig 3d are however not convincing as it appears that there is more signal in treated animals. Also the image seems to be acquired at different times post injection due to signal in the heart chambers. Please clarify.

Reviewer #4 (Remarks to the Author):

It is unfortunate that testing the approach in a model with more developed atherosclerotic lesions was not possible. However, I commend the authors for their well-argued responses to my other queries. One additional concern has arisen from the new presentation of the TUNEL data.

Major Point:

Please review the TUNEL staining results and quantification. The approximately 10% TUNEL+/DAPI+ ratio appears notably high. Typically, in other studies of atherosclerosis in minipigs and humans (e.g., Sukhanov et al., JCI Insight, 2023;8:e165713 and Lutgens et al., Cardiovasc Res, 1999;41:473-9), this ratio has been less than 1%. It seems counterintuitive that 10% of all cell nuclei should exhibit evidence of apoptosis, especially in early atherosclerosis, where defects in efferocytosis are not generally thought to be severe, at least in mice (e.g., Gautier et al., Circulation, 2009;119:1795-804).